CITY COLLEGE
CITY UNIVERSITY OF NEW YORK

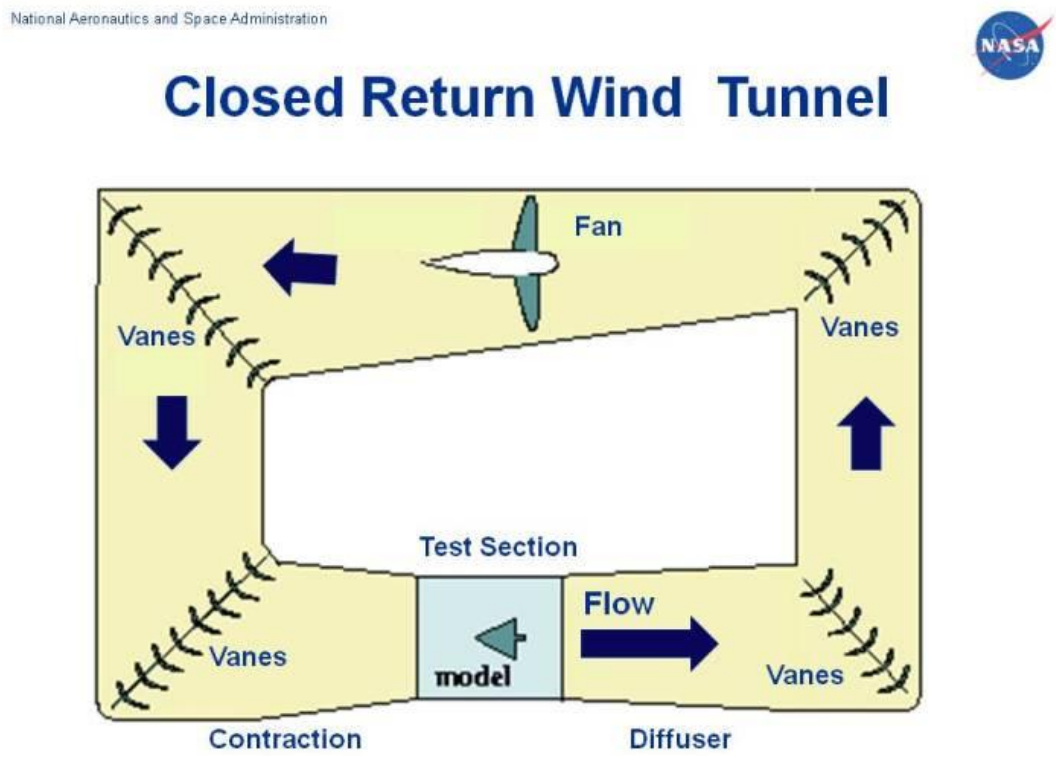

Computational Model of Closed Loop Wind Tunnel

ME G0200 Applied Fluid Mechanics

Fall 2016

Dr. Oleg Goushcha

Submitted by: Pradip Thapa

December 21, 2016

ABSTRACT

In this project, a detailed Computational Fluid Dynamics (CFD) investigation of a closed looped wind tunnel was carried to characterize the fluid flow pattern and pressure drop in a wind tunnel, especially highlighting the effect of turning vanes profile to flow uniformity of air in test section and the resulting pressure drop across the 90 degree turning vanes. A computational methodology for modeling flow conditions in a closed-loop wind tunnel was developed and a full-scale CFD model of the actual wind tunnel was considered for the study. The study was carried out using ANSYS FLUENT to perform CFD study and generate data to study the effect of different vane shapes geometry in flow uniformity and pressure loss. The performance of the wind tunnel designed was calculated through CFD-based simulation but no experiments were conducted to correlate the simulation data. However, the data collected from the simulation results indicate that a uniform flow is maintained in the test section as desired by the streamlined body such as airfoil NACA 6215 with least corner turning pressure loss and provide least overall turbulence intensity in test section.

TABLE OF CONTENTS

1. Introduction

Wind tunnels generate uniform air flow with low turbulence intensity or thermal, aerodynamic and hydraulic testing. Wind tunnels are made in different shapes and sizes, from just 30 cm long to large enough to contain a passenger airplane. There are two basic kinds of wind tunnels, one is the open type which draw its air from the ambient and exits it back to the ambient. Second type of wind tunnel is the closed loop wind tunnel, whose internal air circulated in a loop, separating it from outside ambient air. This kind of wind tunnel requires additional cost for effective temperature control. The temperature in a closed loop win tunnel can be controlled using a combination of heater and heat exchangers.

In general, closed loop wind tunnels are made with the following sections:

1. Test section
2. Settling Chamber
3. Contraction Area
4. Diffuser
5. Blower/Fan Assembly
6. Heat Exchangers
7. Duct and Conner Elbow

A good quality wind tunnel will have a flow uniformity of 0.5-2% and turbulence intensity of 0.5-2%. To achieve uniform, high quality flow in the test section the settling chamber and contraction area are used to smooth the flow. The role of settling chamber, which is upstream of the contraction area, is to eliminate swirl and unsteadiness from the flow. Corners are design with guide vanes to reduce sharp angle variation. Wind tunnels are a significant research apparatus used in aerodynamic investigations to study the effects of air moving past solid objects. In order to avoid the high expenditure of design and adaptation, CFD is often used to precisely comprehend the flow profiles within the tunnel environment. The common objective for most wind tunnels is to obtain a flow in the test section that is a parallel steady flow with uniform speed throughout the test section with least turbulent intensity [1].

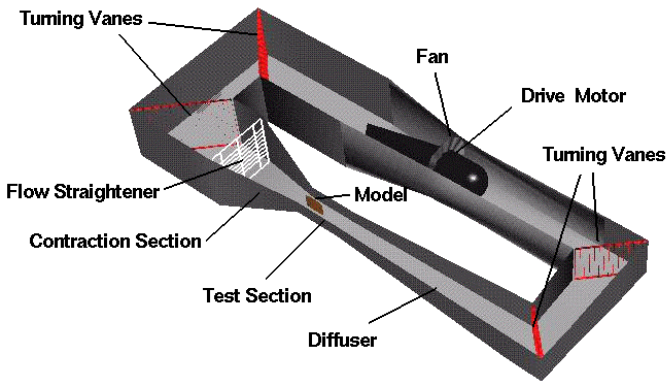

Figure 1.0 Schematic of Closed Loop Wind Tunnel

2. Problem Statement

The wind tunnel for this study is a low speed closed-loop wind tunnel that have an overall path length of 168 ft. with a test section of the height, width, and length of 3 ft., 3ft. and 6ft. respectively. The tunnel operated as closed circuit in which air that passes through the test section was drawn back into the fan and re-circulated into the test section repeatedly. Guide vanes were used to turn the airflow around the corners of the wind tunnel while minimizing the turbulence and power loss. The CFD study will be carried out using ANSYS FLUENT for different vane shapes geometry for flow direction inside the wind tunnel turns. Then, the studies will be compare to design a wind tunnel that will generate a uniform air flow of **35 m/s** with a low turbulence intensity for testing.

3. Geometry

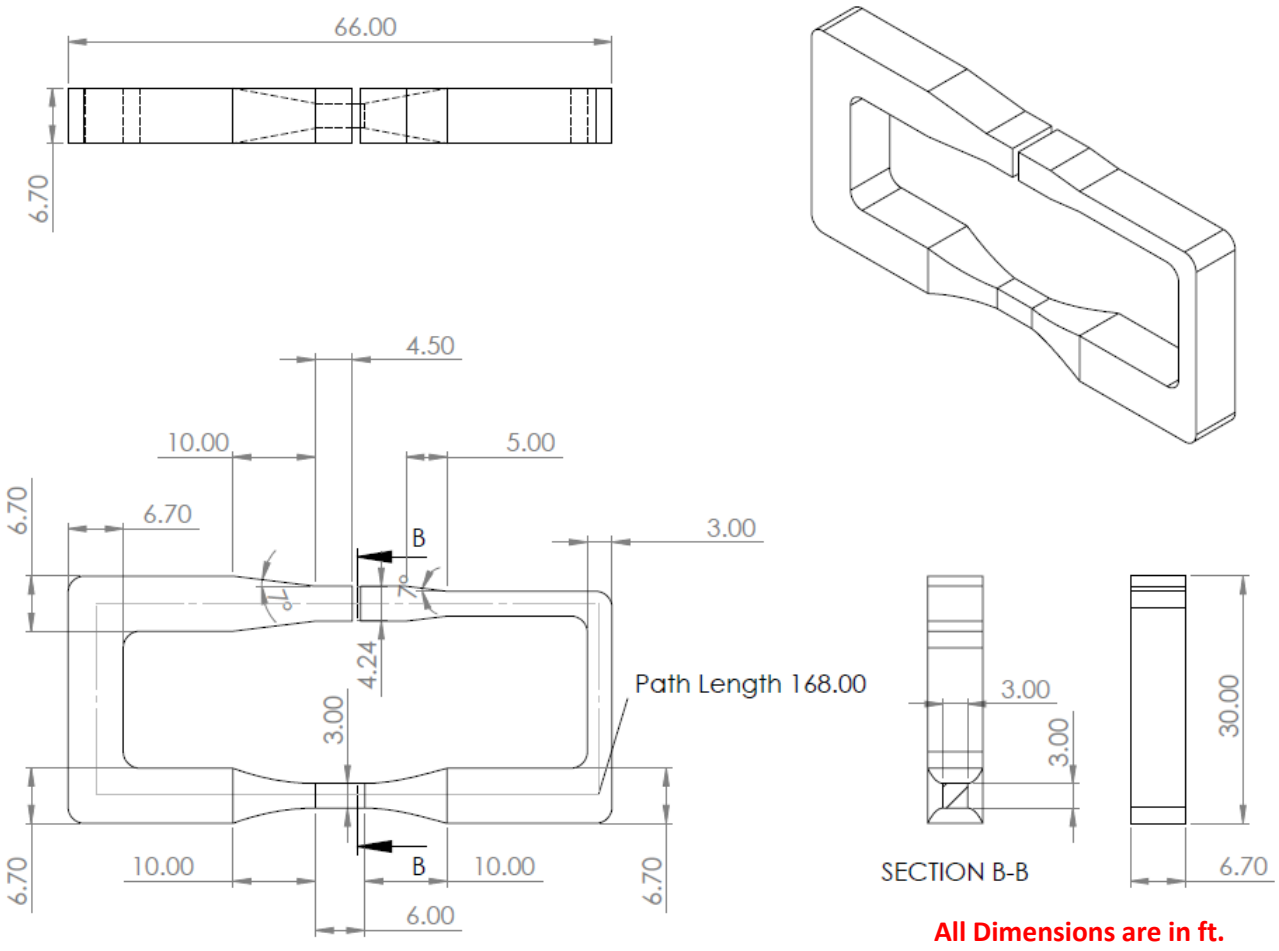

Figure 2.0 Dimension Drawing of Closed Loop Wind Tunnel without Vanes

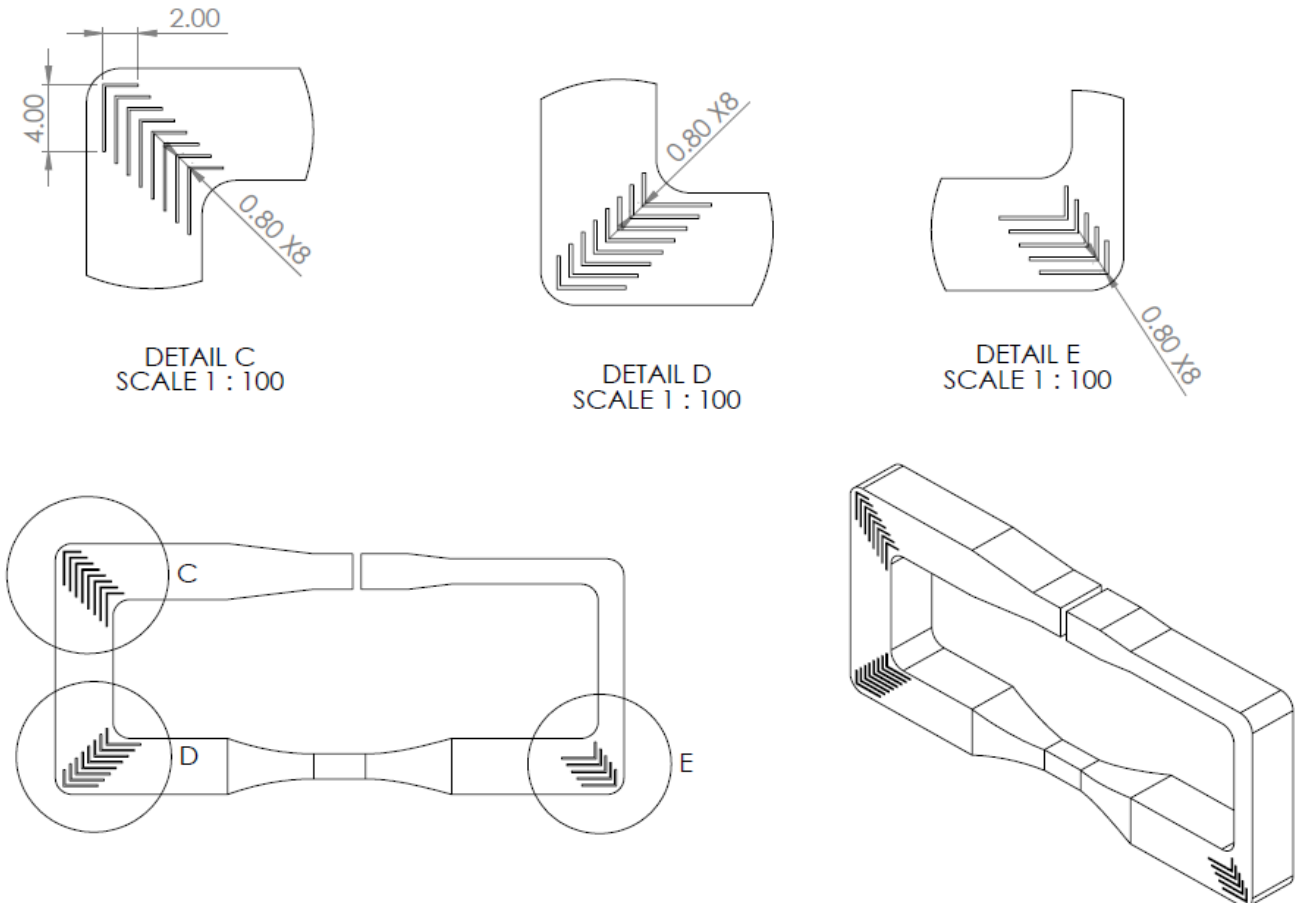

Figure 3.0 Dimension Drawing of Closed Loop Wind Tunnel with 90 deg. Vanes

It is well known that for abrupt rectangular corners, large aspect ratios and larges ratios of turning radius to inlet width are required to reduce the corner loss. This has led to the post-second world war concept of closely spaced turning vanes to provide low loss, compact, wind tunnel corners.

In the past, it has been common to use thick profile airfoil turning vanes because these can be designed to give air turning passages of approximately constant area, thus avoiding any expansion and possible flow separation around the passage between adjacent turning vanes. Such turning vanes are efficient in operation, but very difficult and expensive to construct.

Additionally, in this project we will conduct the study of two additional guide vanes design with the guideless based on NASA research “Aerodynamic Design Guidelines and Computer Program for Estimation of Subsonic Wind Tunnel Performance”. As in closed loop wind tunnel flow must be deflected by 90° four times with minimum turbulence at the four corners. Efficient and effective blade and bent are critical in design overall performance. The best chord-to-gap ratio depends on the vane type. For thick vanes, a ratio of about 2-to-1 is recommended and for thin vanes a ratio of about 4-to-1 is suggested [2].

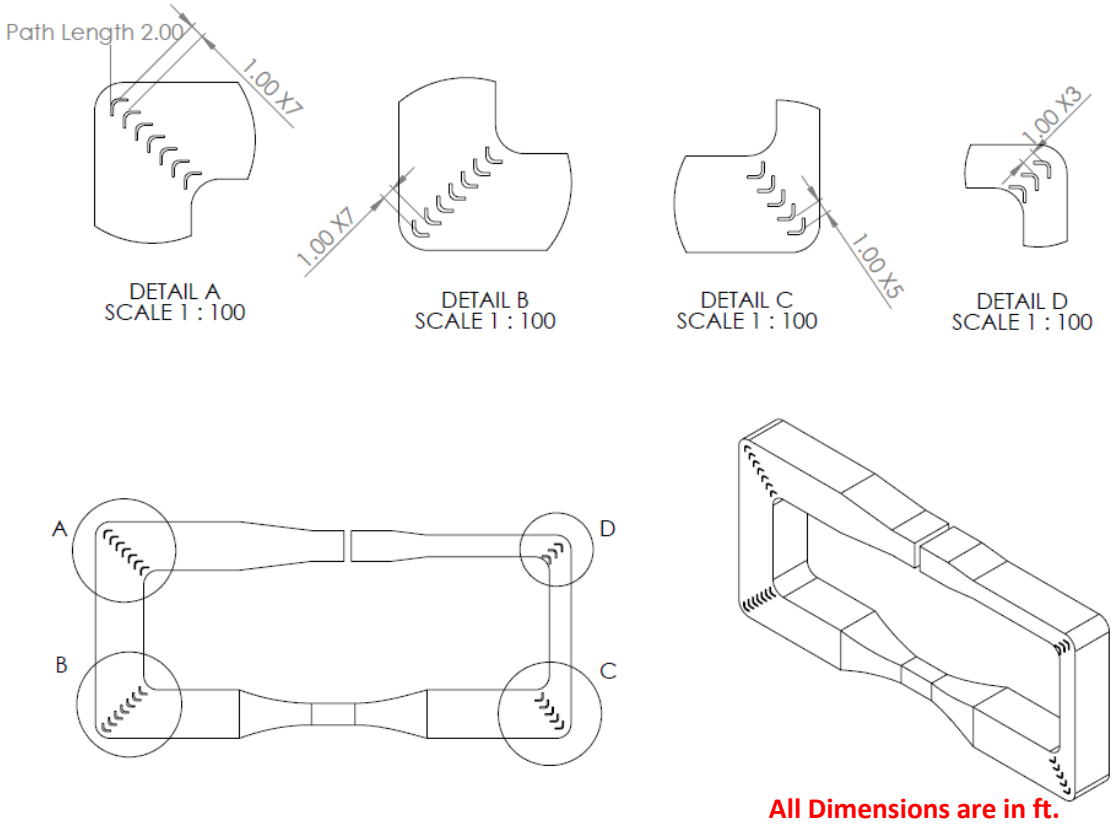

Figure 4.0 Dimension Drawing of Closed Loop Wind Tunnel with C Vanes

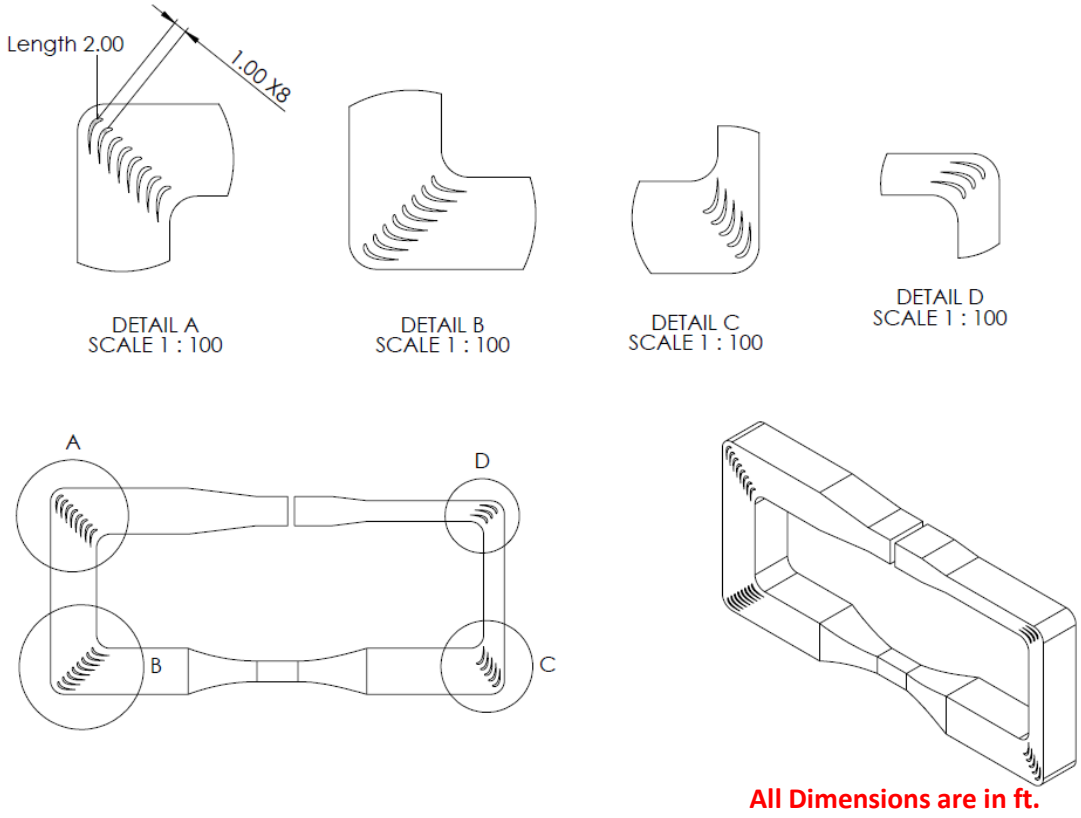

Figure 5.0 Dimension Drawing of Closed Loop Wind Tunnel with NACA 6215 Airfoil Vanes

4. Mesh

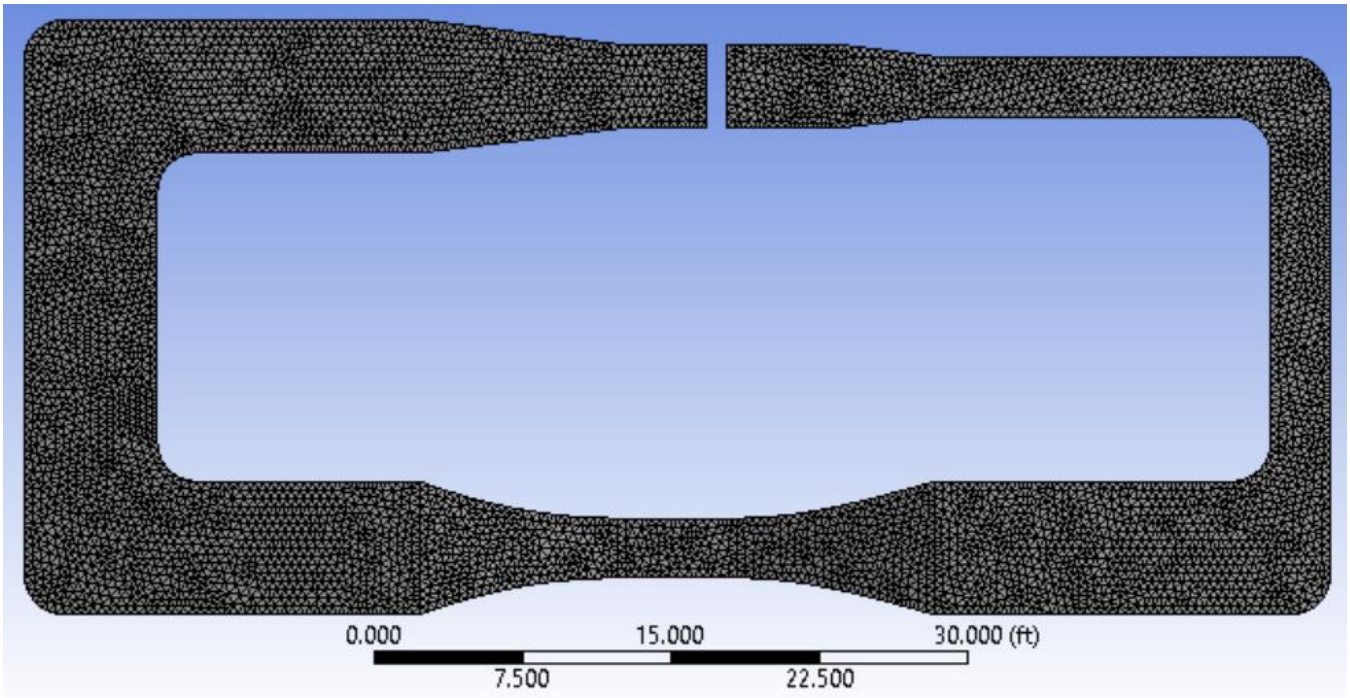

Figure 6.0 Meshed Geometry Closed Loop Wind Tunnel without Vanes

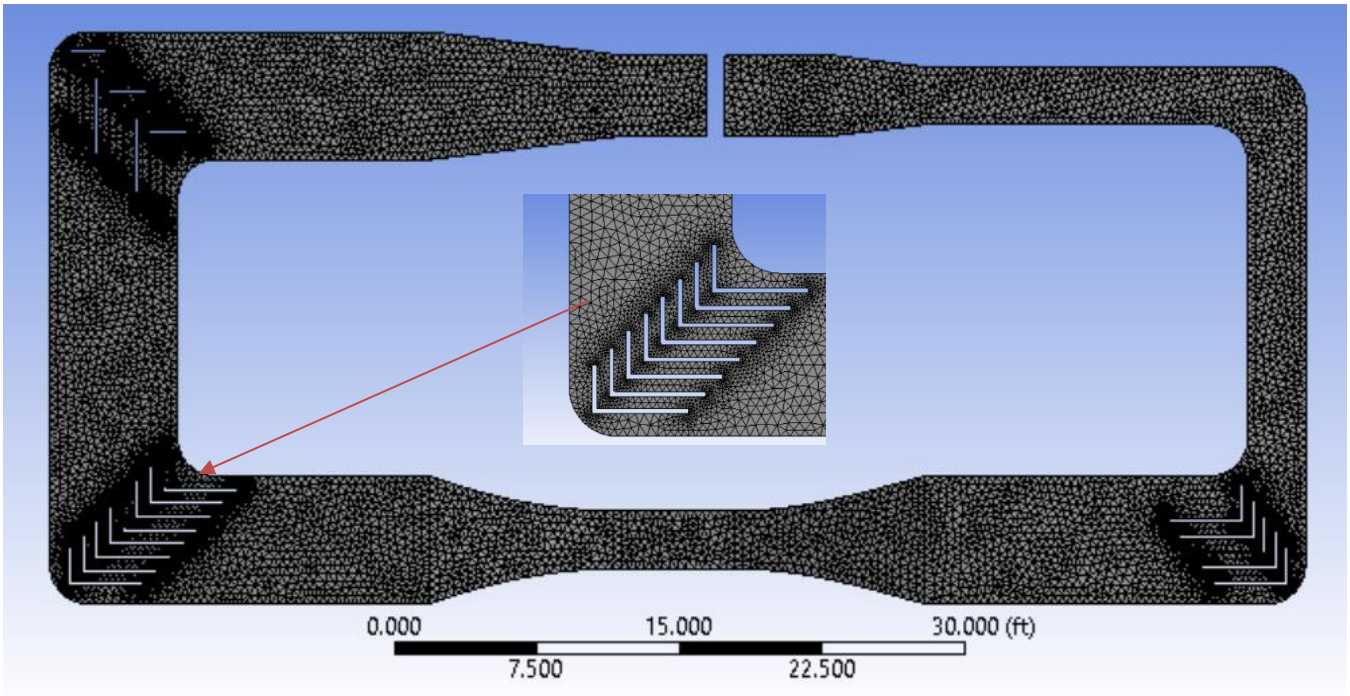

Figure 7.0 Meshed Geometry Closed Loop Wind Tunnel with 90 deg. Vanes

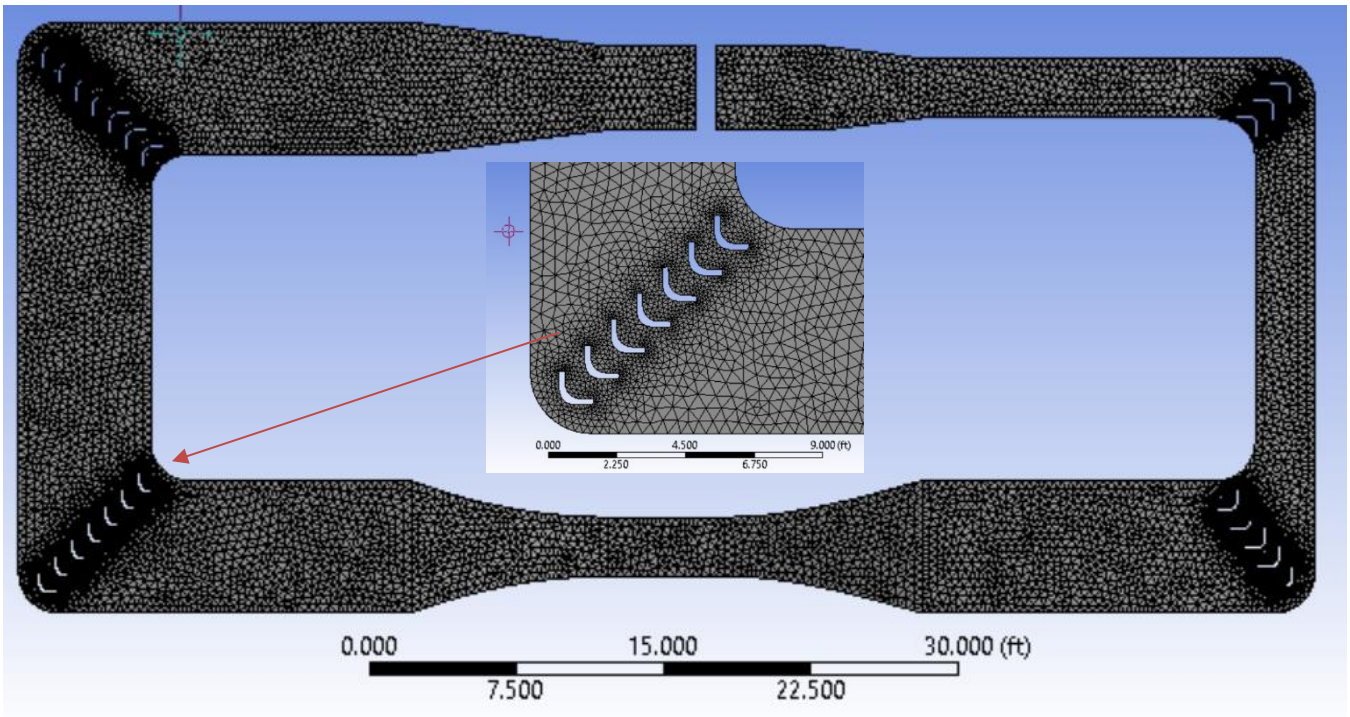

Figure 8.0 Meshed Geometry Closed Loop Wind Tunnel with C Vanes

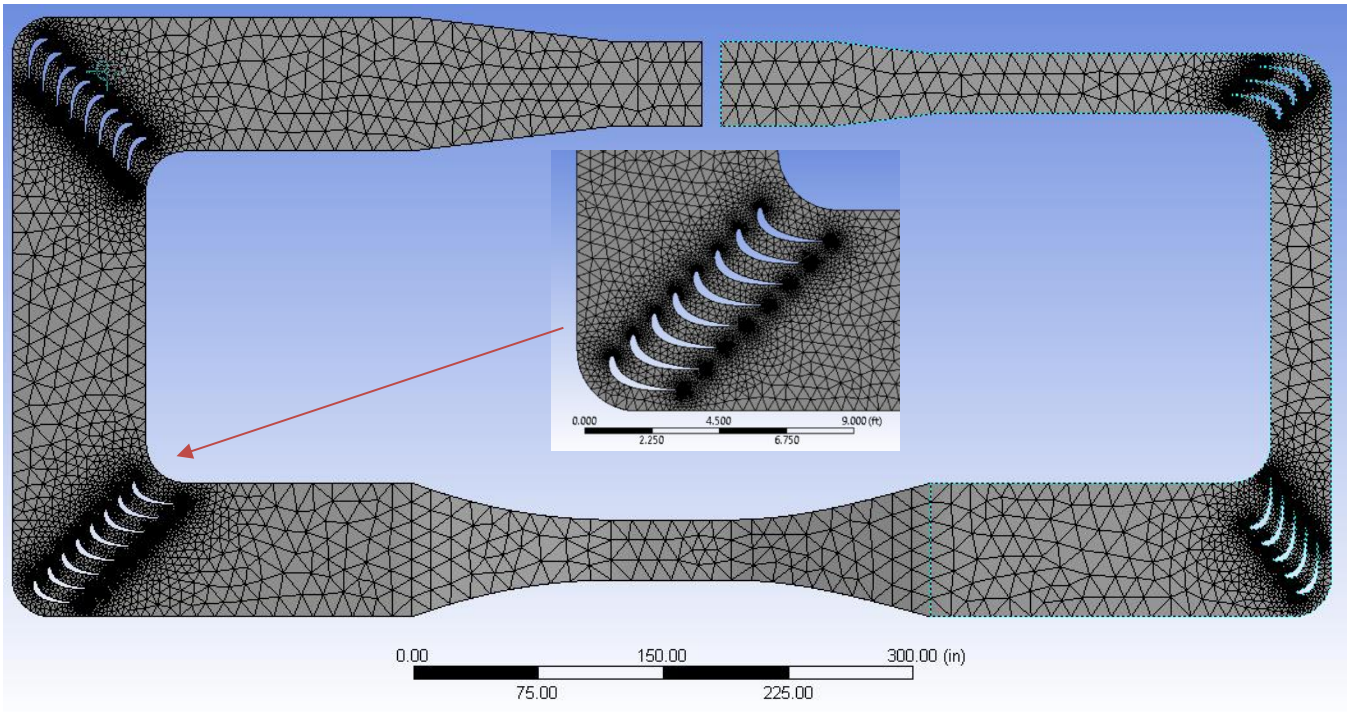

Figure 9.0 Meshed Geometry Closed Loop Wind Tunnel with NACA 6215 Airfoil Vanes

Due to mesh failure for case number 4, the maximum element size was increase to 12 to reduce number of elements and min size was reduced to 0.1 to match the minimum tolerance of geometry curvature. This caused the total calculation time of 8hrs for Fluent solver to perform 100 iterations.

Table 1.0 Summary of Mesh Properties

Case #	# of Nodes	# of Elements	Max/min size of the mesh elements [inch]	Method
1	122223	658456	[5/1]	Tetrahedrons
2	335805	1743906	[5/1]	Tetrahedrons
3	341366	1823845	[5/1]	Tetrahedrons
4	3184434	17701367	[12/0.1]	Tetrahedrons

5. Boundary conditions

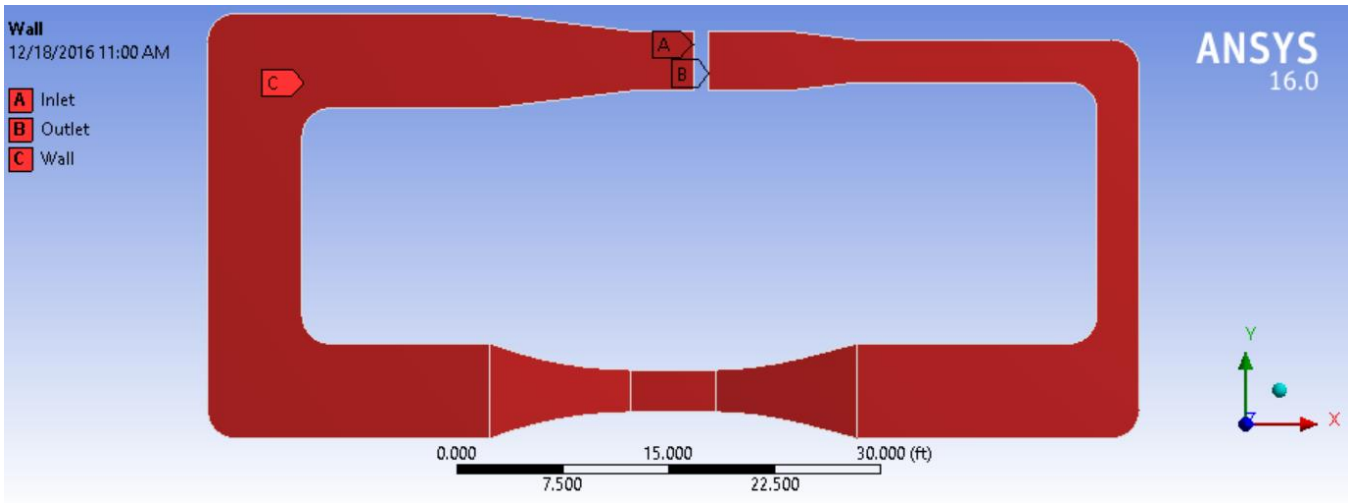

Figure 10.0 Boundary Condition for Closed Loop Wind Tunnel without Vanes

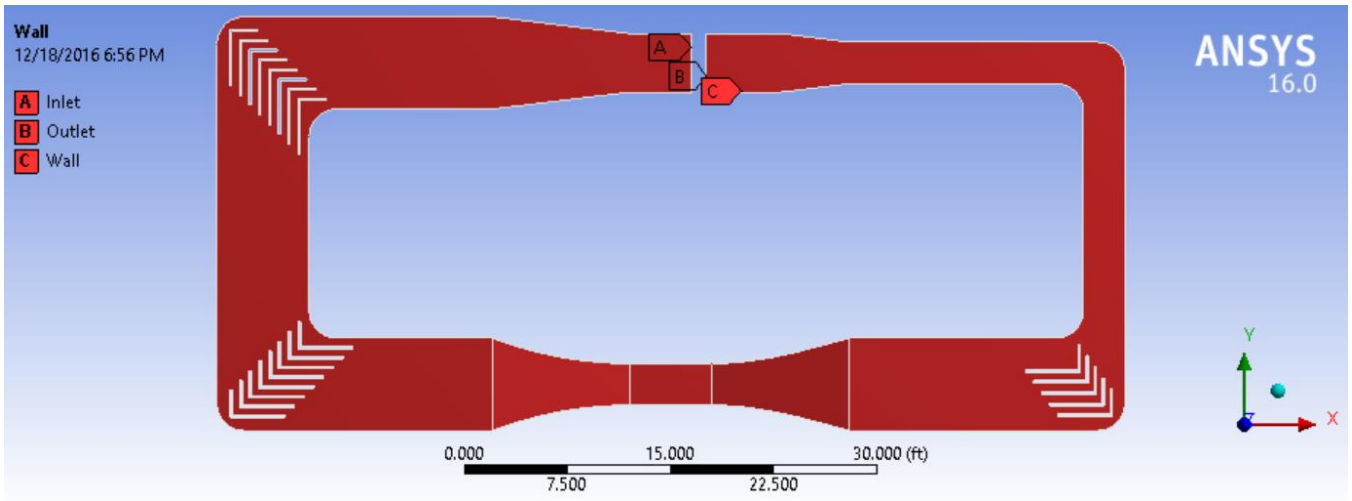

Figure 11. Boundary Condition for Closed Loop Wind Tunnel with 90 deg. Vanes

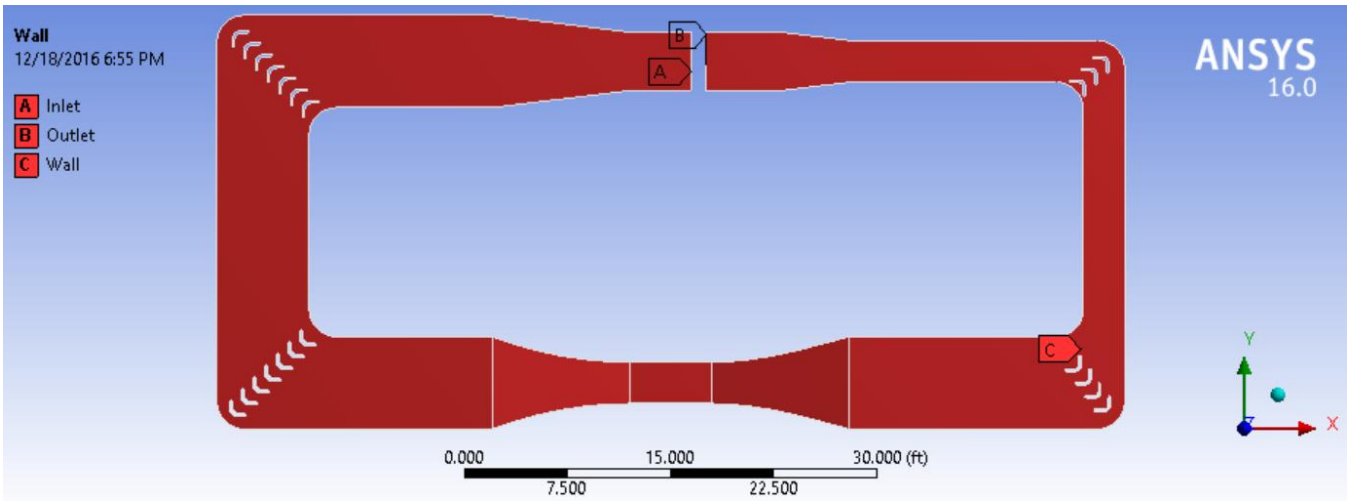

Figure 12.0 Boundary Condition for Closed Loop Wind Tunnel with C Vanes

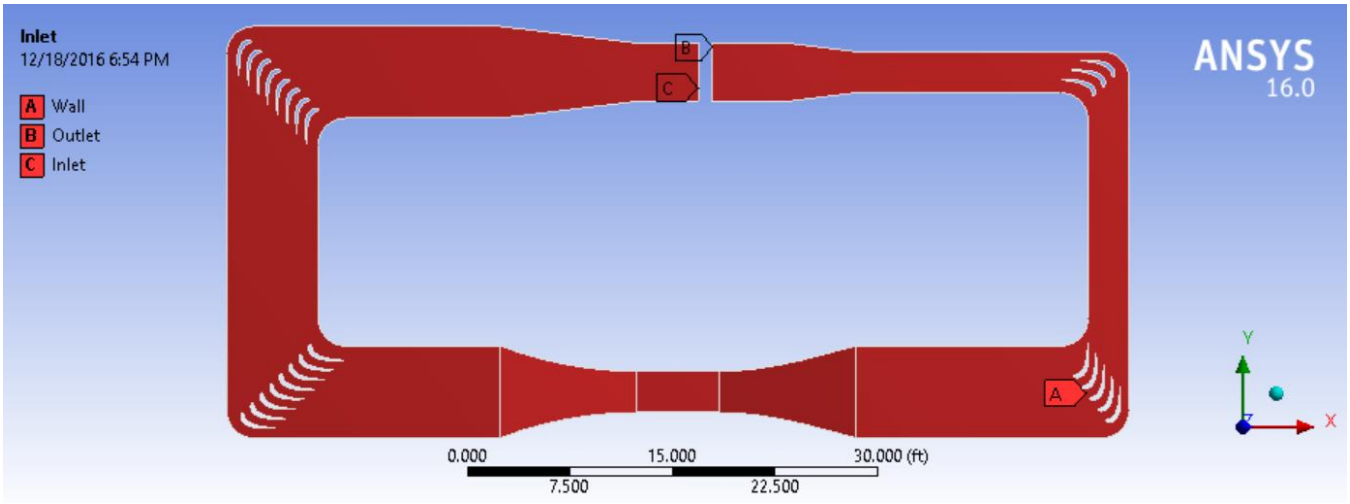

Figure 13.0 Boundary Condition for Closed Loop Wind Tunnel with NACA 6215 Airfoil Vanes

Using name selections tools three distinction non over lapping surface boundary names were create before importing the model into Fluent. This was very effective tool for defining parameter within Fluent GUI and also during post process for results and data.

Boundary Surface are

- All external surface as wall of Tunnel and surface of vanes
- Inlet Surface to simulate fan/blower.
- Outlet Surface for solver to convergence. Even though it is a close loop wind tunnel, inlet-outlet boundary condition was assumed to simplify the approach.

6. Setup

6.1 Calculation

$$Reynolds\ Number\ (Re_{H_d}) = \frac{\rho * U * D_H}{\mu}$$

$$D_H = \frac{4A}{P} = \frac{4 * 3 * 3}{2 * (3 + 3)} = 3\ [ft] = 0.9144\ [m]$$

$$U = 35\ \left[\frac{m}{s}\right]$$

$$\rho = 1.225\ \left[\frac{kg}{m^3}\right]$$

$$\mu = 1.7894 * 10^{-5}\left[\frac{kg}{m-s}\right]$$

$$(Re_{H_d}) = \frac{1.225 * 35 * 0.9144}{1.7894 * 10^{-5}} = \mathbf{2190952}$$

To study our model, we decide the use Turbulent flow k-epsilon model because we know, for internal flow, if the Reynolds number is greater than 2300, flow is turbulent and to get correct approximation of flow behavior from CFD, we need correct solver method to solve the governing equations.

6.2 Model

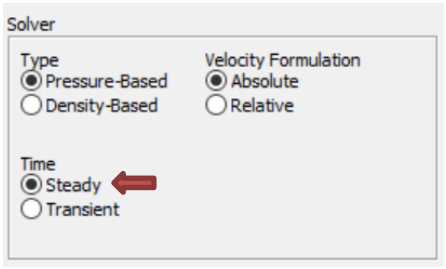

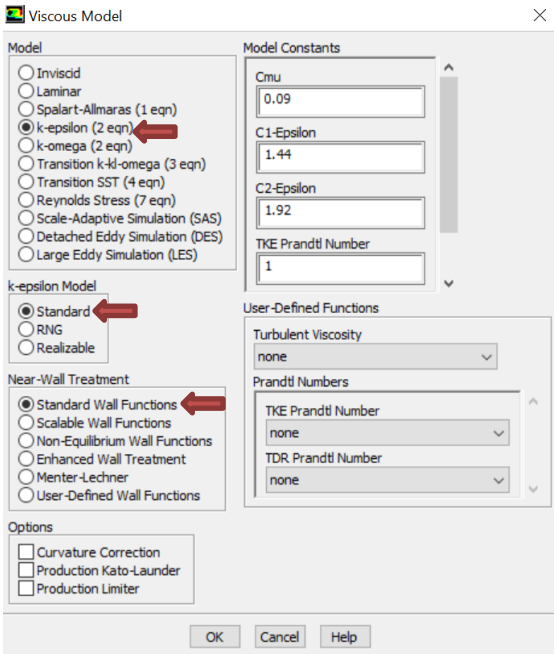

6.3 Material

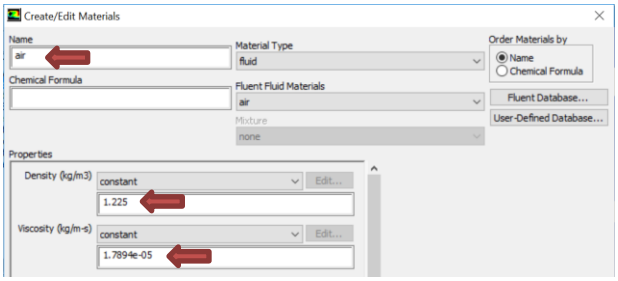

6.4 Boundary Conditions

Using continuity equation for constant mass flow rate,

$$A_1V_1 = A_2V_2$$

$$(3 * 3)[ft^2] * 35\left[\frac{m}{s}\right] = (4.24 * 6.7)[ft^2] * V_2$$

$$V_2 = \frac{3*3}{(4.24*6.7)} * 35\ \left[\frac{m}{s}\right] = \mathbf{11.08}\ \left[\frac{m}{s}\right]$$

- Inlet Boundary Condition is $\mathbf{11.08}\ \left[\frac{m}{s}\right]$
- Outlet Boundary Condition is $\mathbf{0}\ [\boldsymbol{Pa}]$
- Wall Boundary Condition is ***No slip condition***

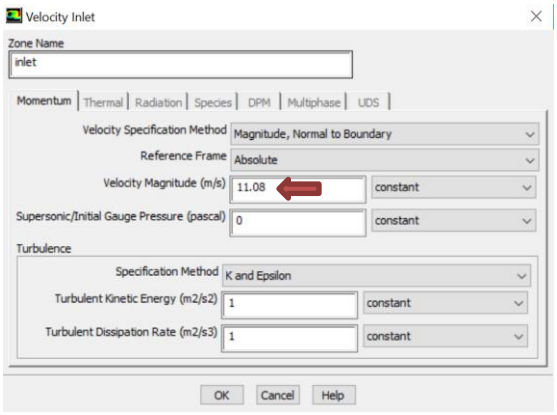

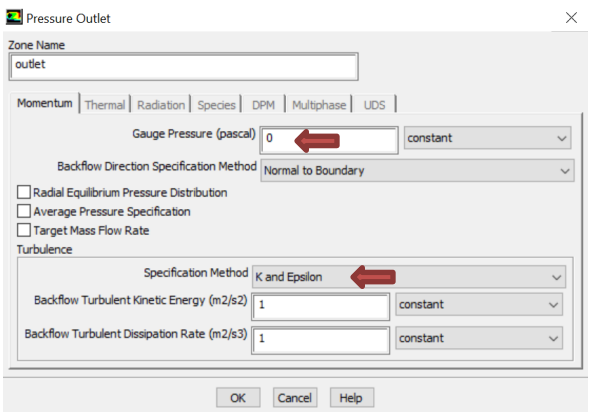

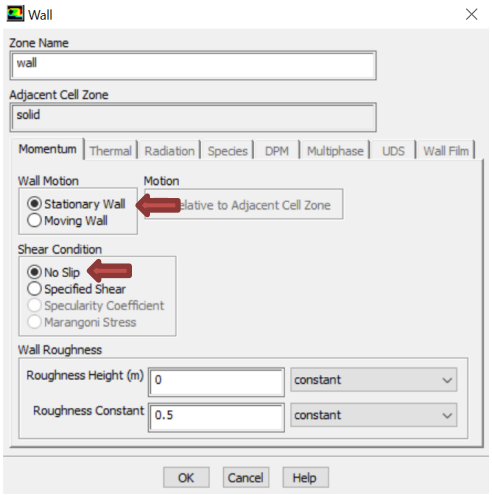

6.5 References and Initialization Value

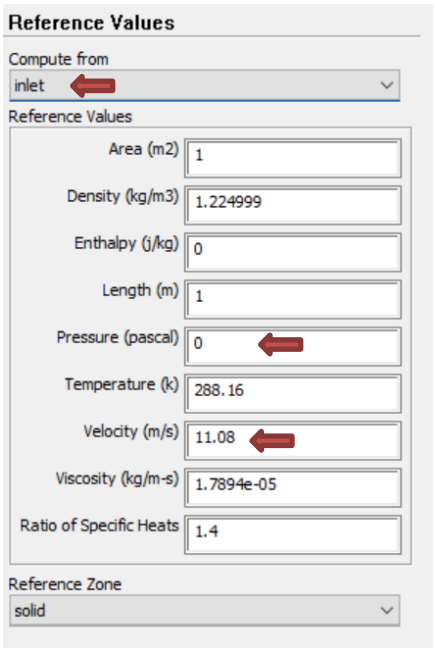

6.6 Convergence and Calculation

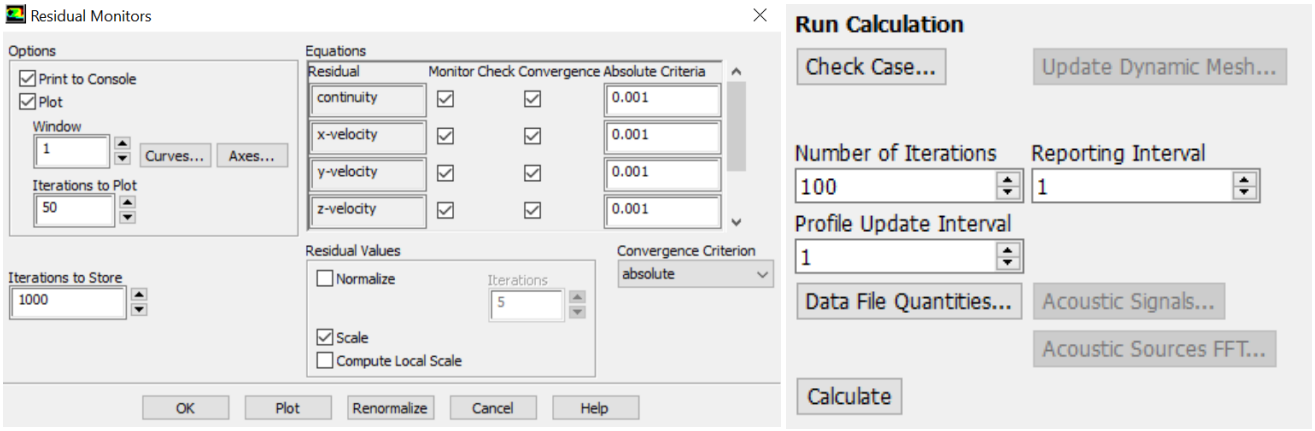

The Standard K-Epsilon model (SKE) is the most widely-used engineering turbulence model for industrial applications and is one of the most common turbulence models. It is a two-equation model, that means, it includes two extra transport equations to represent the turbulent properties of the flow. This allows a two-equation model to account for history effects like convection and diffusion of turbulent energy. The first transported variable is turbulent kinetic energy, k and the second transported variable is the turbulent dissipation, ε. It is the variable that determines the scale of the turbulence, whereas the first variable, k, determines the energy in the turbulence.

7 Results

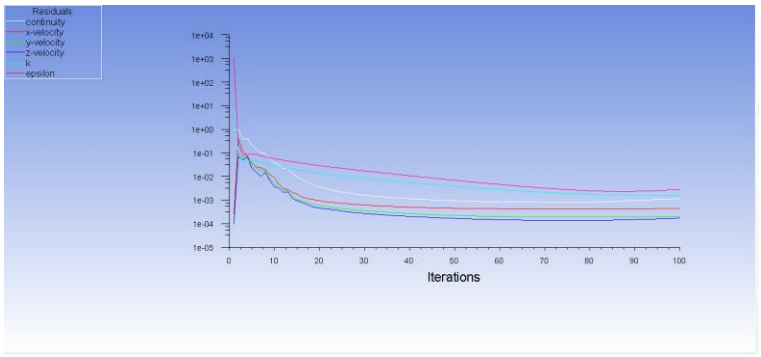

Figure 14.0 Residual Plot for Closed Loop Wind Tunnel without Vanes

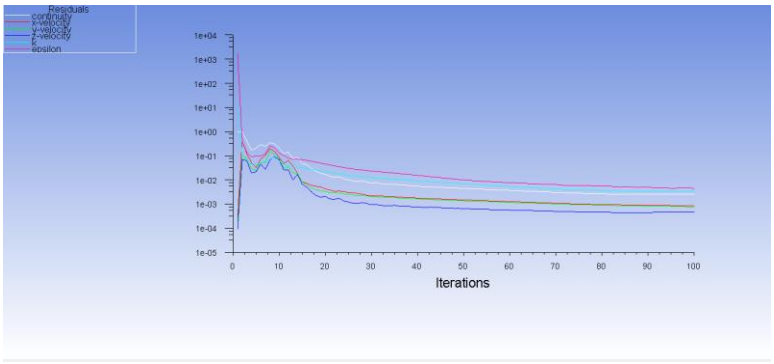

Figure 15.0 Residual Plot for Closed Loop Wind Tunnel with 90 deg. Vanes

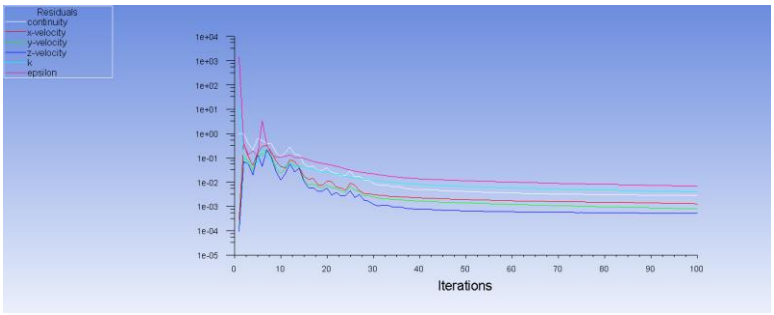

Figure 16.0 Residual Plot for Closed Loop Wind Tunnel with C Vanes

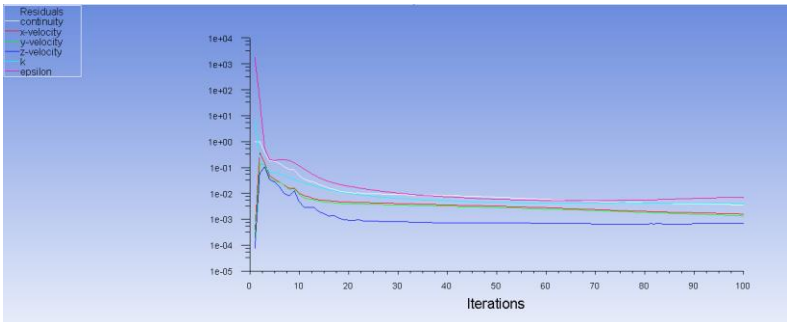

Figure 17.0 Residual Plot for Closed Loop Wind Tunnel with NACA 6215 Airfoil Vanes

Calculation were based on reference values from inlet and the due to high number of elements and large model domain the number of iteration was set to 100. A convergence results were obtained for all scenarios.

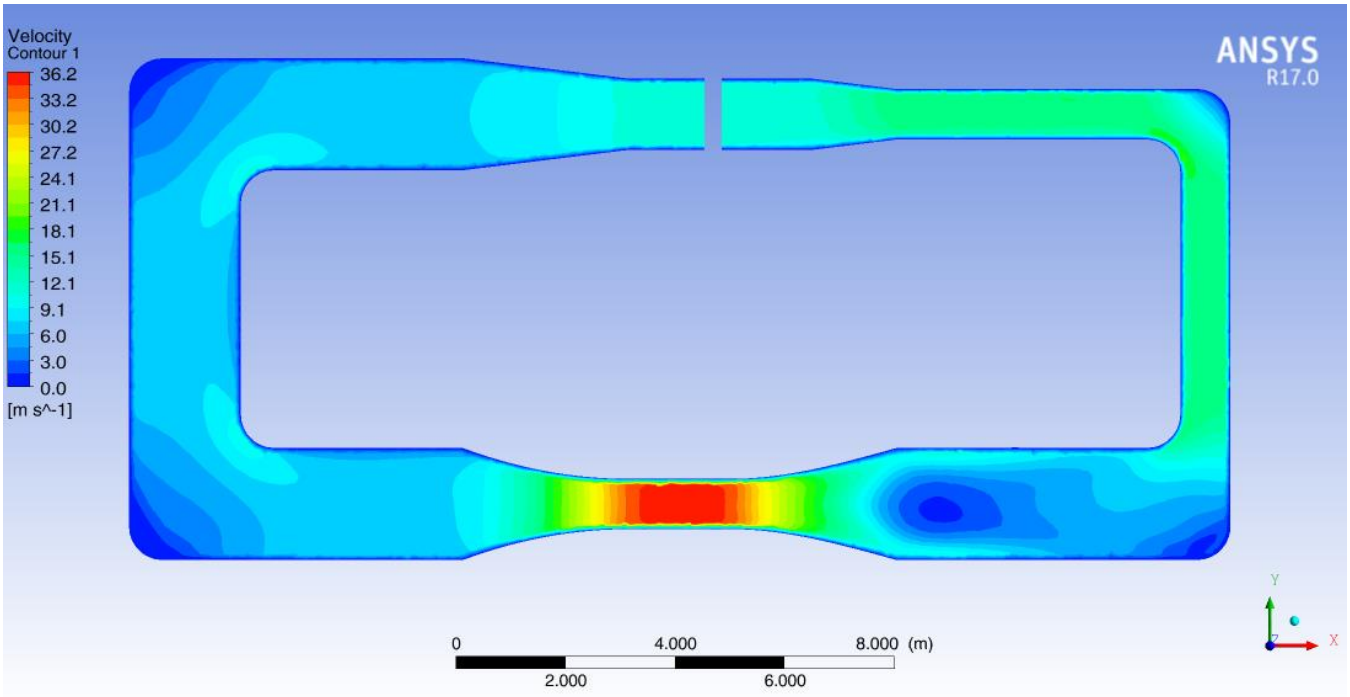

Figure 18.0 Velocity Plot for Closed Loop Wind Tunnel without Vane

As expected flow stagnation is observed at the in the 90 deg. turning corner. Even though contractor and expansion before and after the test section was not significantly design for this project it was observed that there is a flow stagnating right after the expansion.

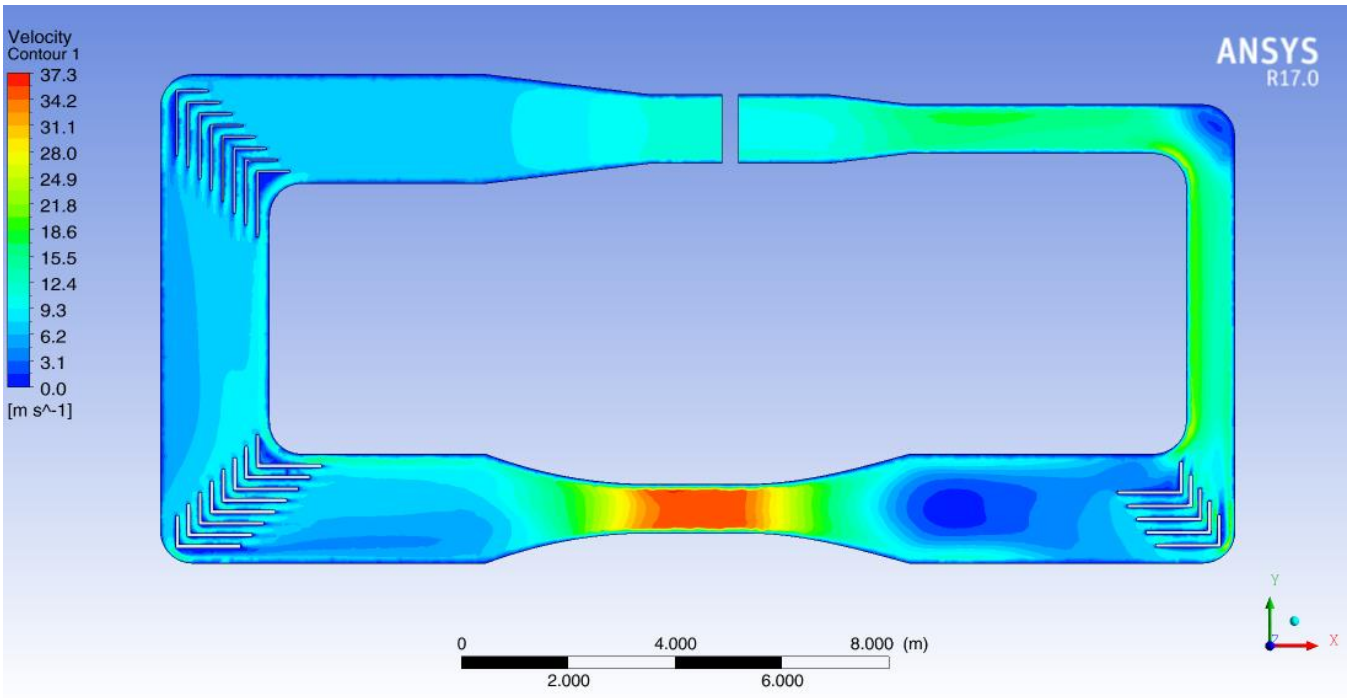

Figure 19.0 Velocity Plot for Closed Loop Wind Tunnel with 90 deg. Vanes

The corner flow stagnation is smoothed out by adding the vanes. To differential its effect corner 4 didn't have any vanes and we can see flow stagnation in the figure above.

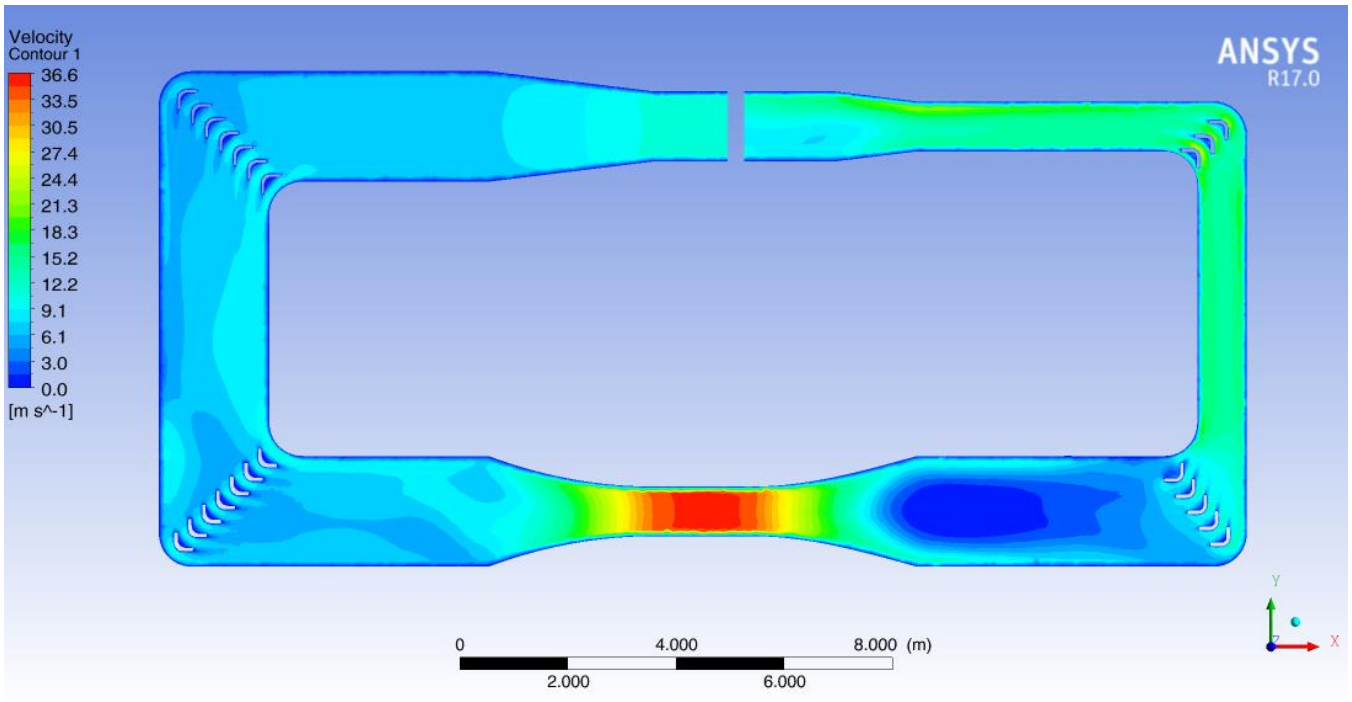

Figure 20.0 Velocity Plot for Closed Loop Wind Tunnel with C Vanes

Case 3 was studied for a 2 ft. path length symmetric C vanes with length to spacing ratio of 2:1. We observed that the flow has smoothed out more effecting however we still observed the stagnation after the flow expansion after test section.

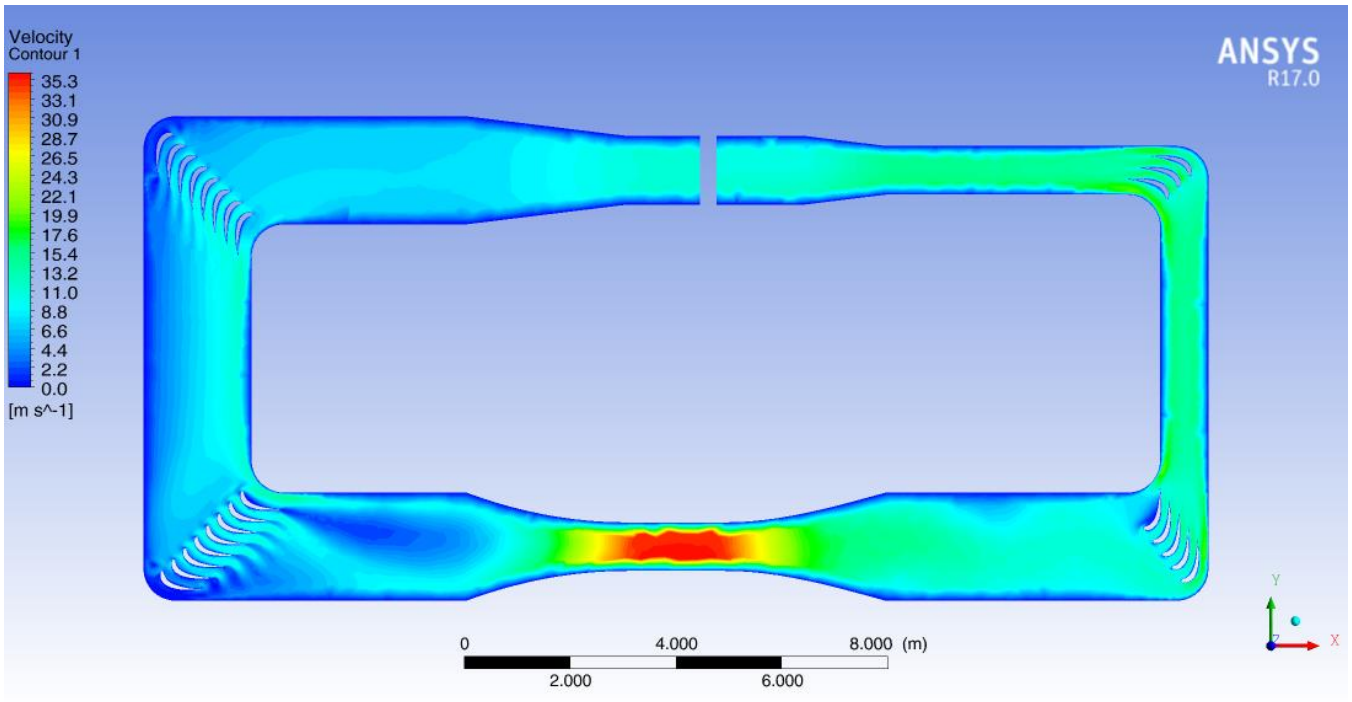

Figure 21.0 Velocity Plot for Closed Loop Wind Tunnel with NACA 6215 Airfoil Vanes

Case 4 was modeled with NACA 6215 airfoil with chord length 2 and chord to space ratio of 2:1. Because of larger element size the actual flow behavior might not have been capture for this model however it gave any interesting result that is airfoil vanes significant supplied desired flow pattern.

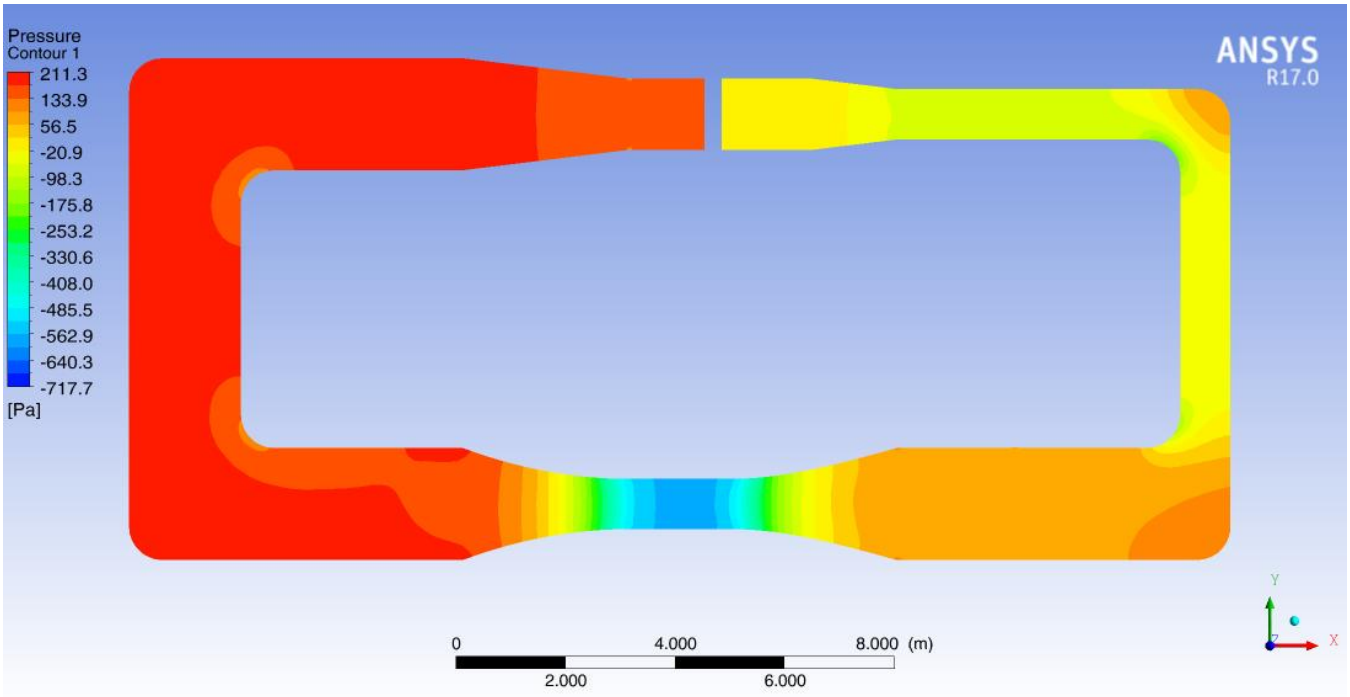

Figure 22.0 Pressure Plot for Closed Loop Wind Tunnel without Vanes

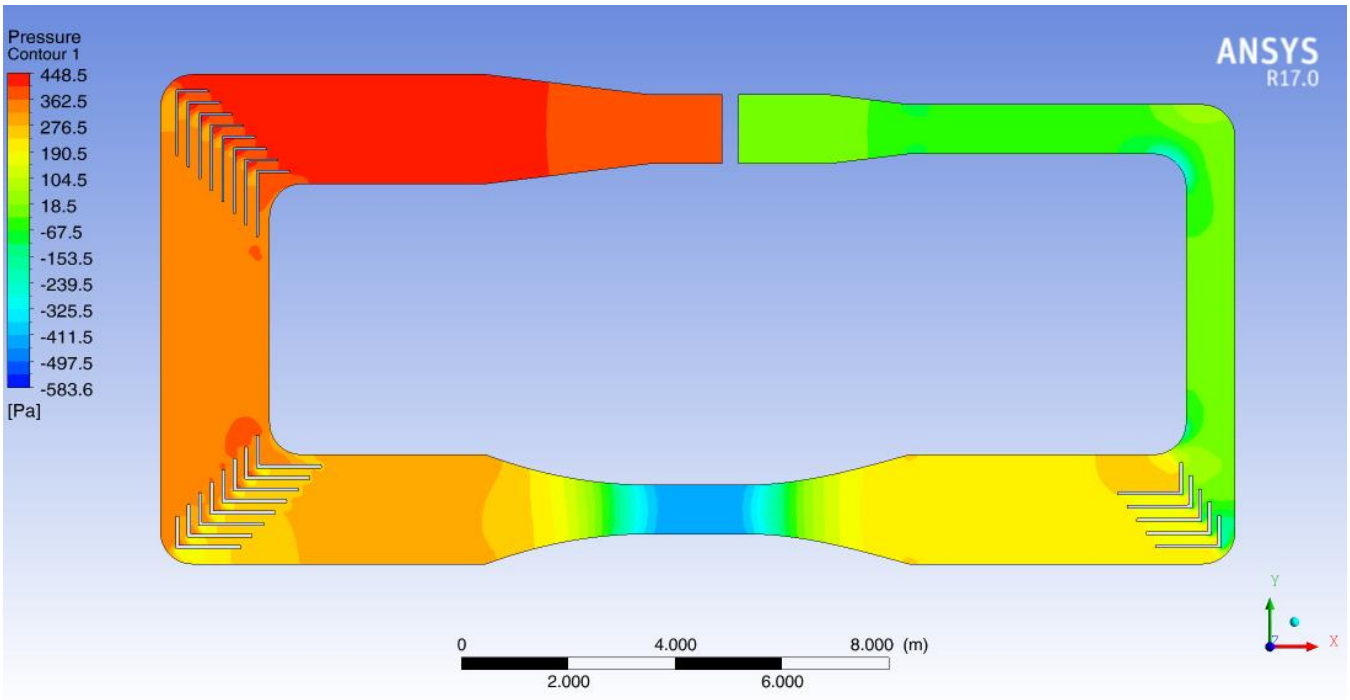

Figure 23.0 Pressure Plot for Closed Loop Wind Tunnel with 90 deg. Vanes

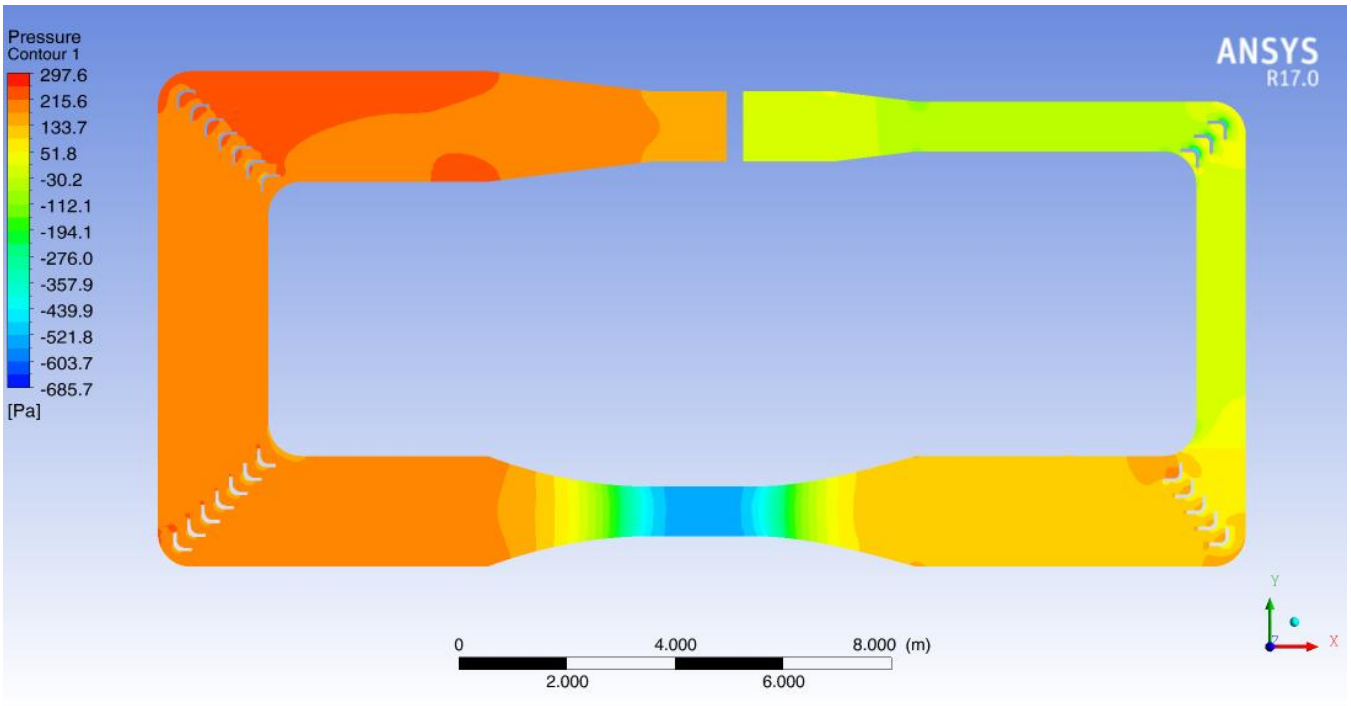

Figure 24.0 Pressure Plot for Closed Loop Wind Tunnel with C Vanes

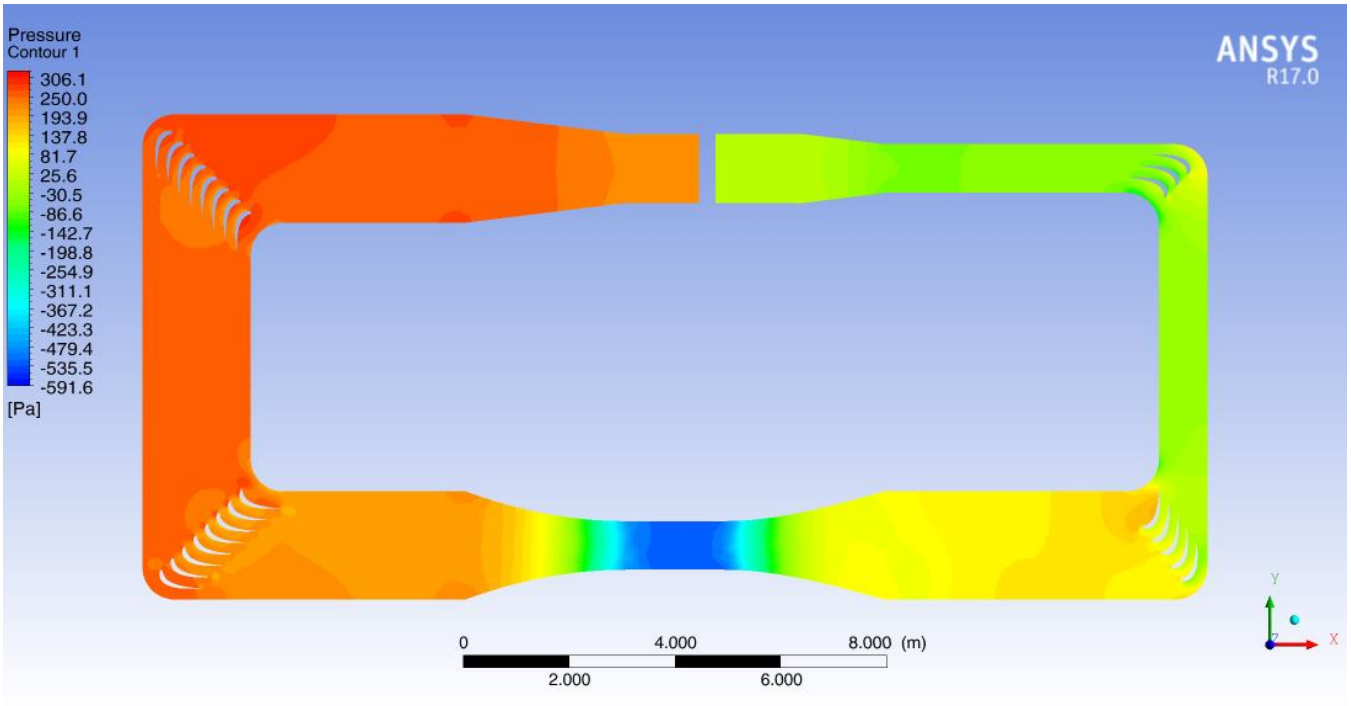

Figure 25.0 Pressure Plot for Closed Loop Wind Tunnel with NACA 6215 Airfoil Vanes

Comparing all four cases, we see that thin and long turning vanes caused significant pressure loss compare to symmetric C vanes and airfoil vanes. It was very hard to evaluate effectively the pressure losses however using probing tools in CFD post processing it was approximated that the pressure losses in corner 1 for case 2, 3 and 4 are 80 Pa, 40Pa and 20 Pa respectively.

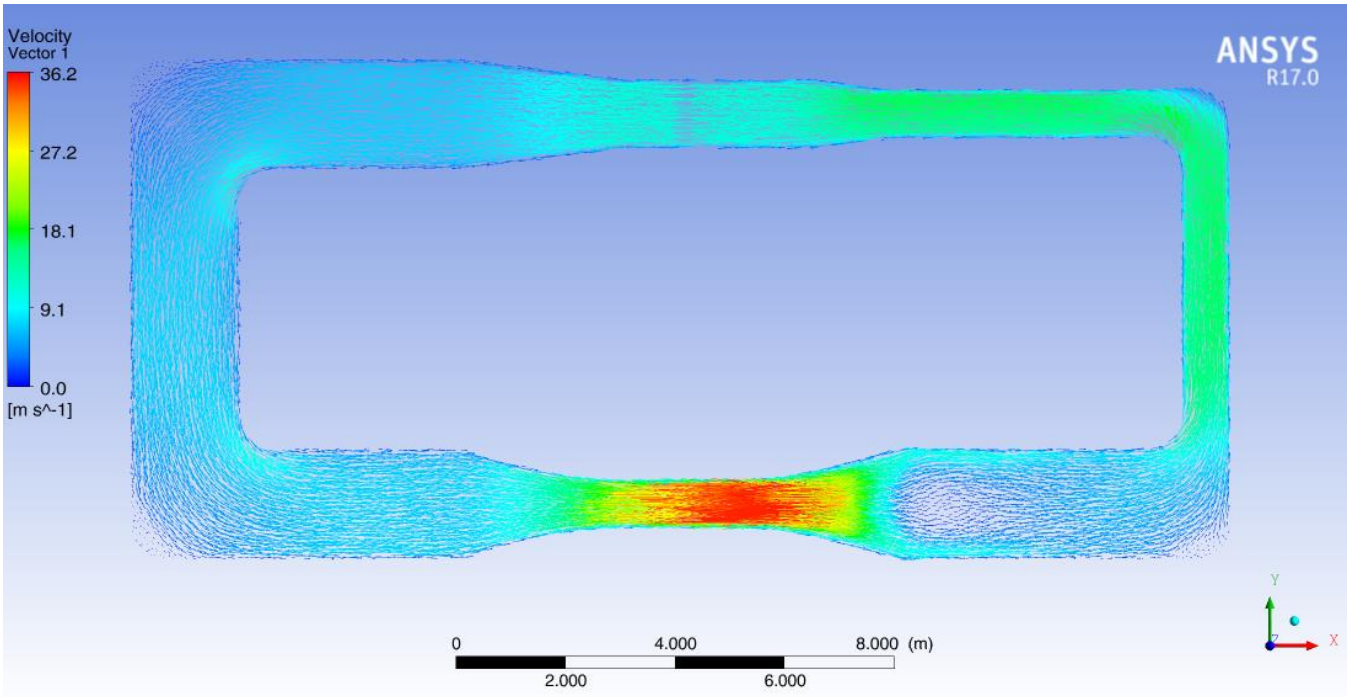

Figure 26.0 Velocity Vector Plot for Closed Loop Wind Tunnel without Vanes

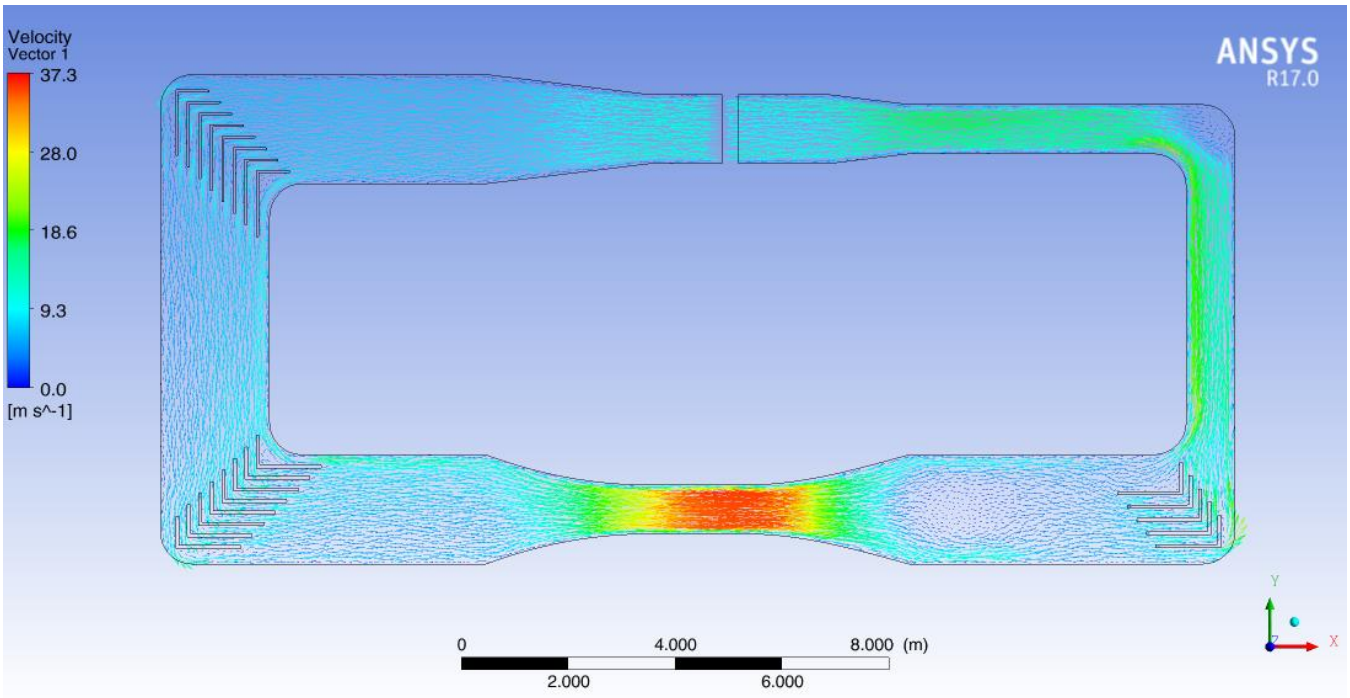

Figure 27.0 Velocity Vector Plot for Closed Loop Wind Tunnel with 90 deg. Vanes

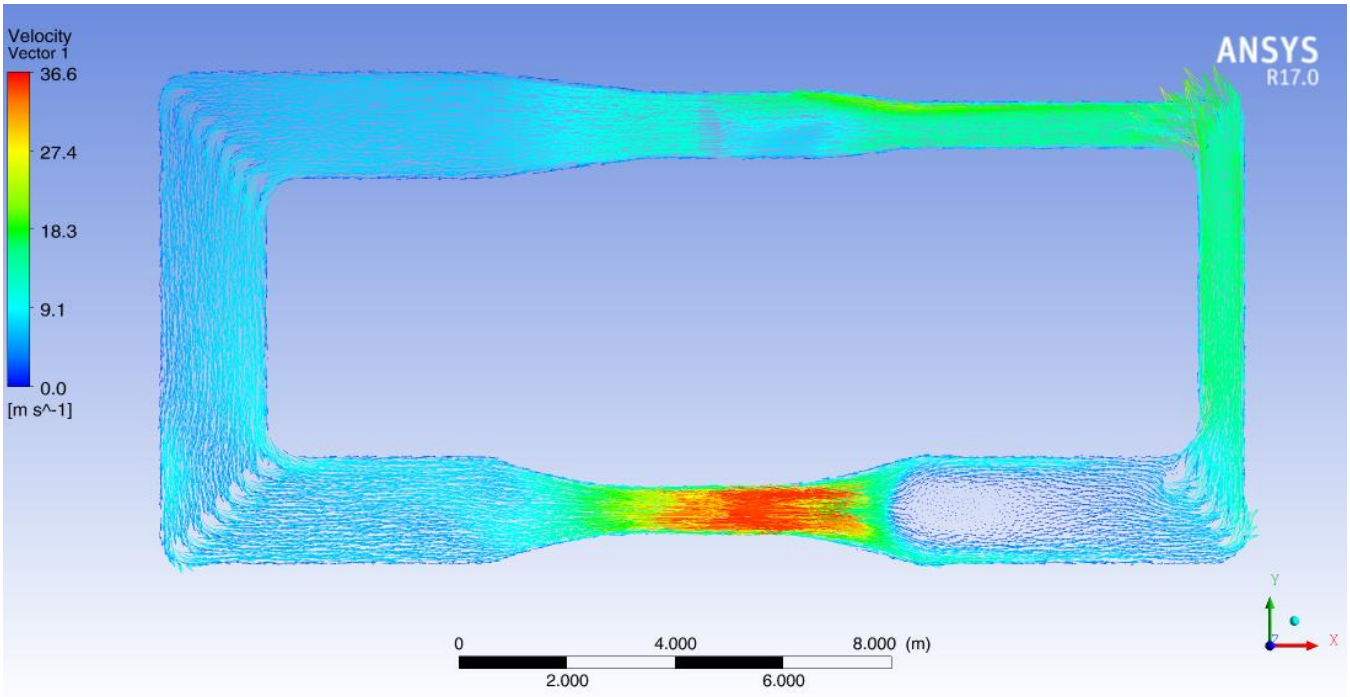

Figure 28.0 Velocity Vector Plot for Closed Loop Wind Tunnel with C Vanes

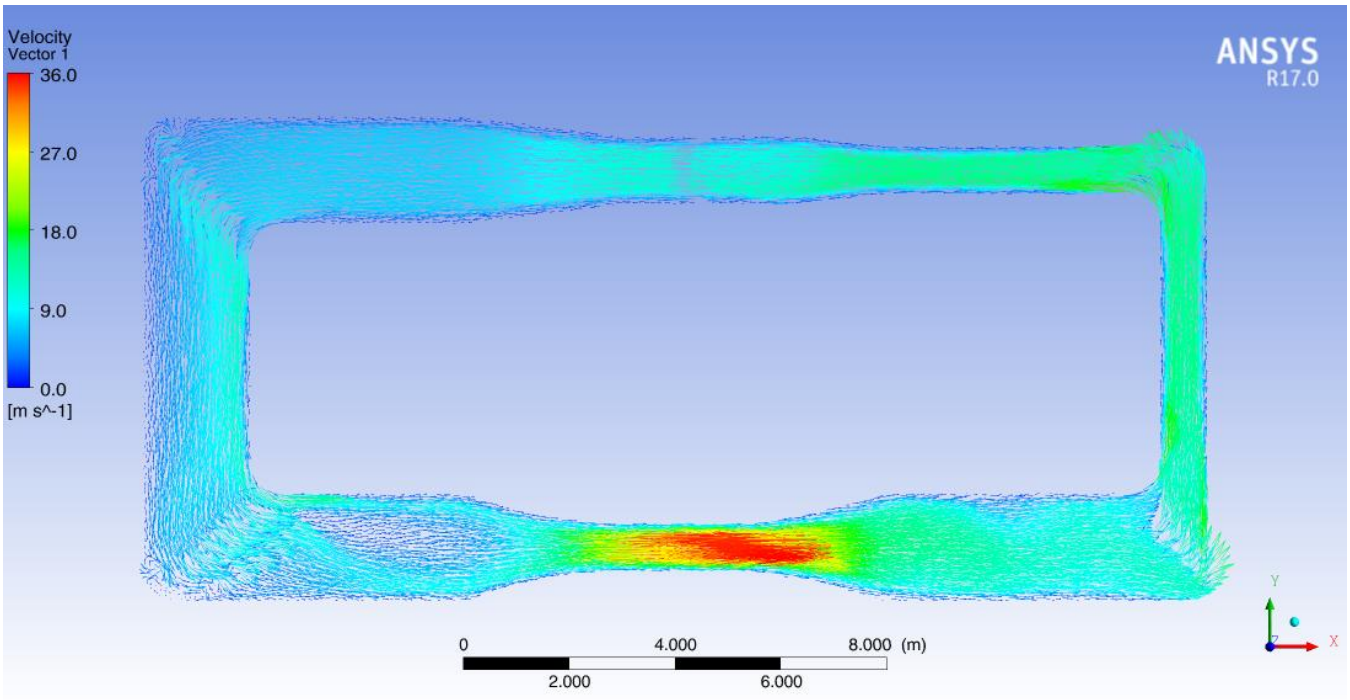

Figure 29.0 Velocity Vector Plot for Closed Loop Wind Tunnel with NACA 6215 Airfoil Vanes

Comparing all four cases vector plot, we see that the wind tunnel without vanes have flow recirculation on the turning corner as well as in the region right after test section expansion. This recirculation is significantly reduced by adding vanes. However, we see some recirculation in the region before the test section which was counter intuitive and further investigation.

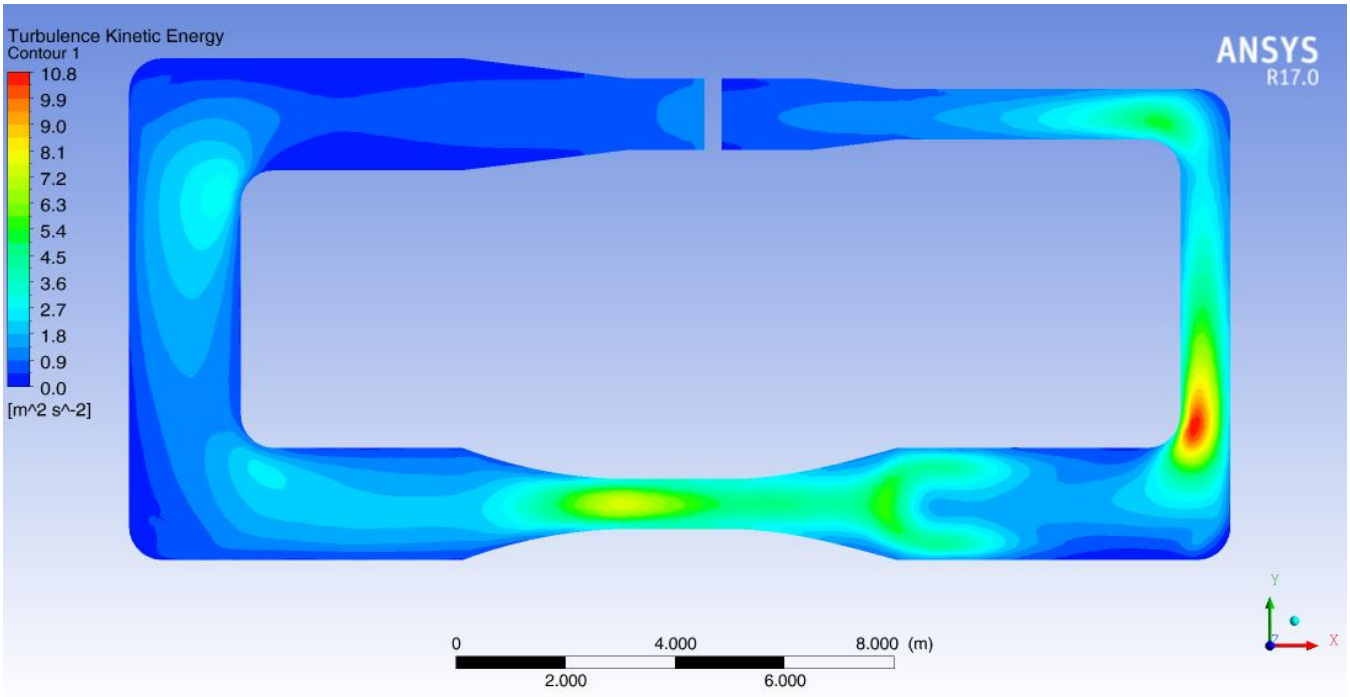

Figure 30.0 Turbulence Kinetic Energy Plot for Closed Loop Wind Tunnel without Vanes

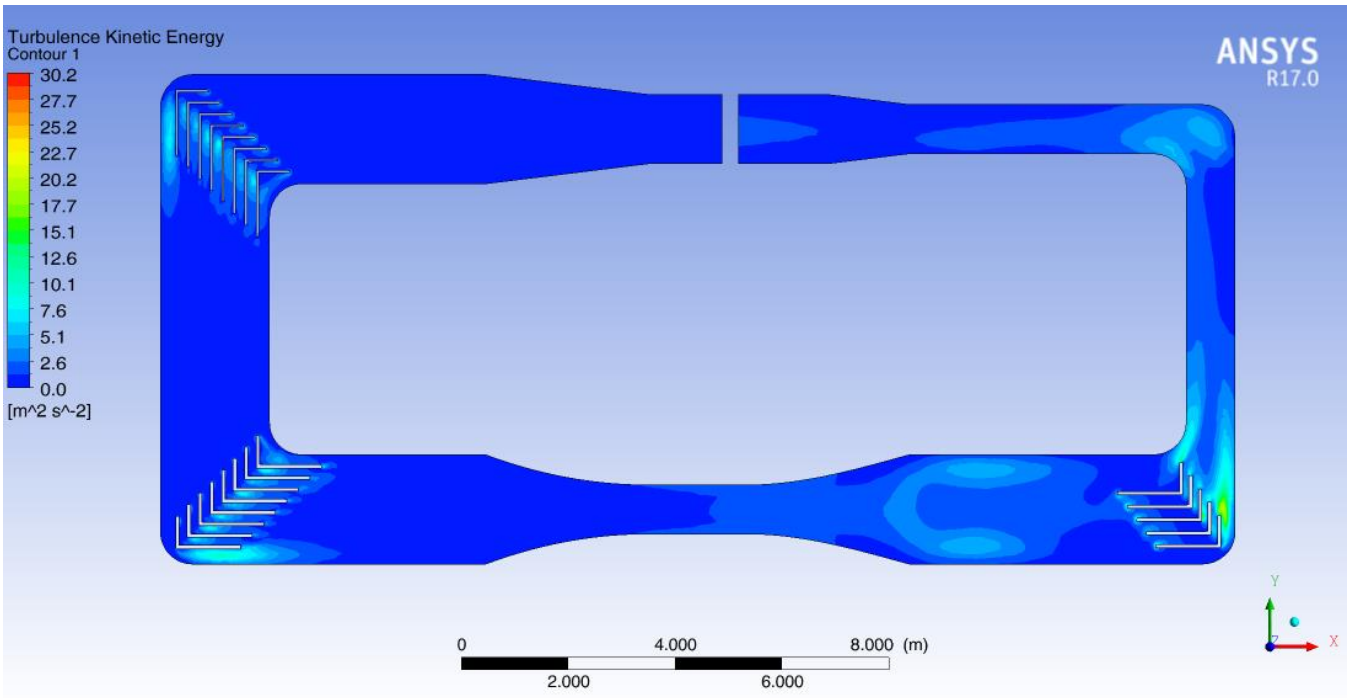

Figure 31.0 Turbulence Kinetic Energy Plot for Closed Loop Wind Tunnel with 90 deg. Vanes

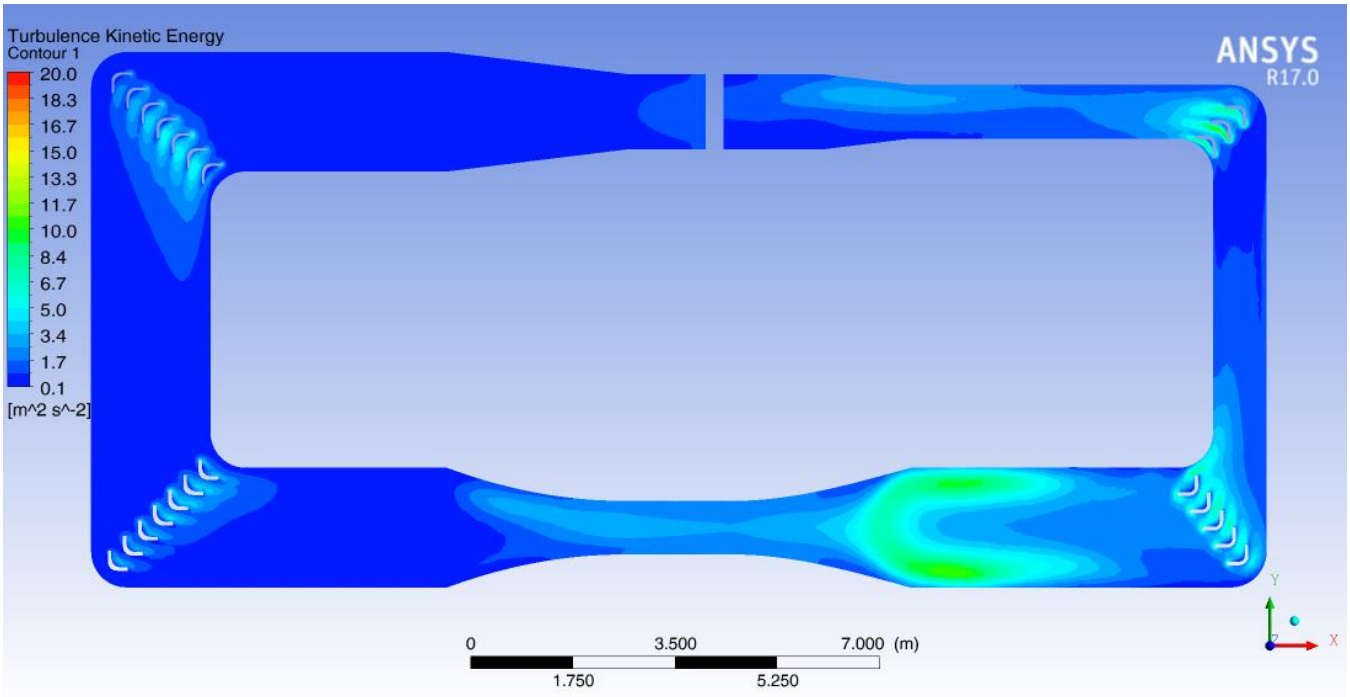

Figure 32.0 Turbulence Kinetic Energy Plot for Closed Loop Wind Tunnel with C Vanes

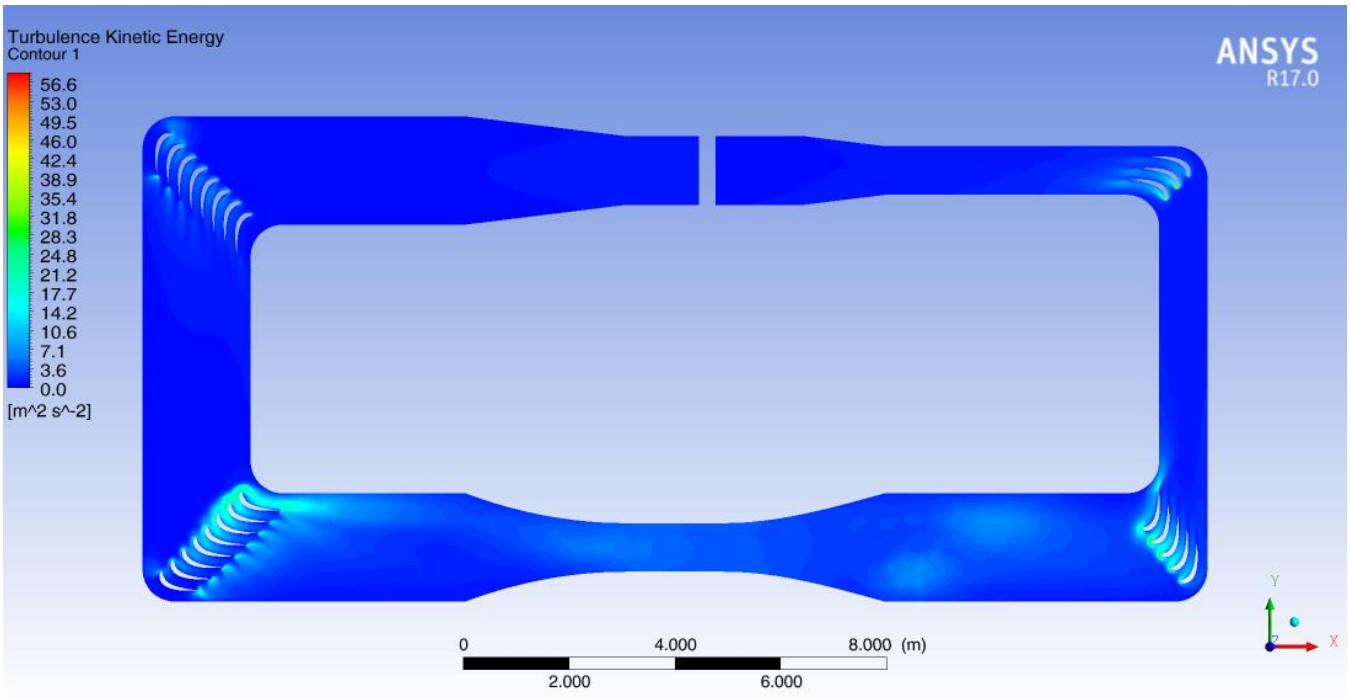

Figure 33.0 Turbulence Kinetic Energy Plot for Closed Loop Wind Tunnel with NACA 6215 Airfoil Vanes

Comparing all four cases, we see that the wind tunnel with airfoil produced the least turbulence kinetic energy in comparison to other three cases. Corner 2,3 and 4 produce some turbulence which could be due to different turning angle and required mesh optimization to capture real flow. However, computation time to solve this model was very time consuming and required large solver memory power.

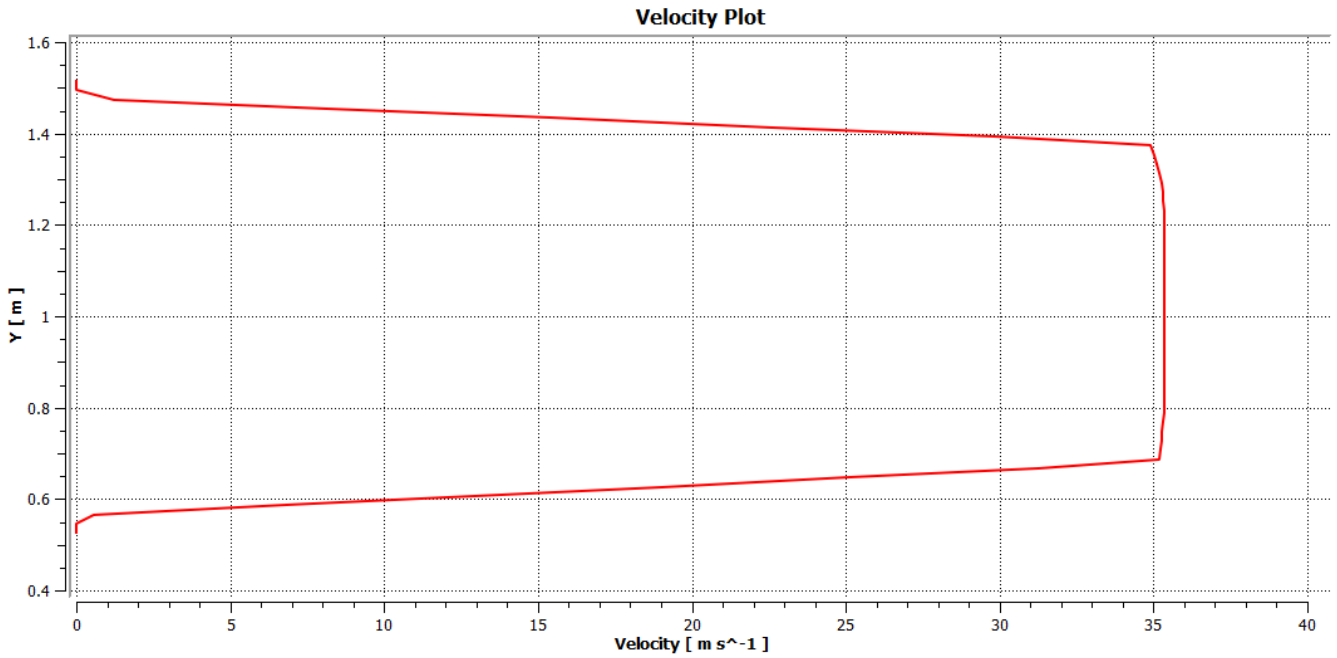

Chart 1.0 Velocity Distribution in Test Section for Closed Loop Wind Tunnel without Vanes

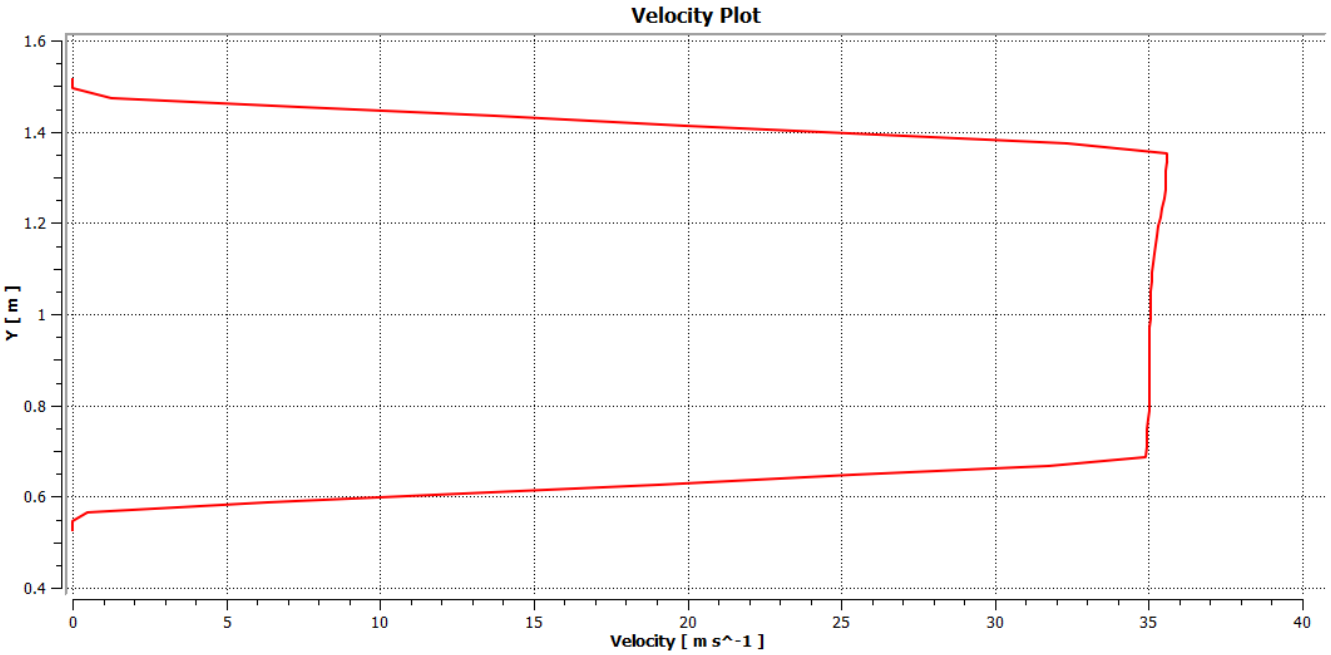

Chart 2.0 Velocity Distribution in Test Section for Closed Loop Wind Tunnel with 90 deg. Vanes

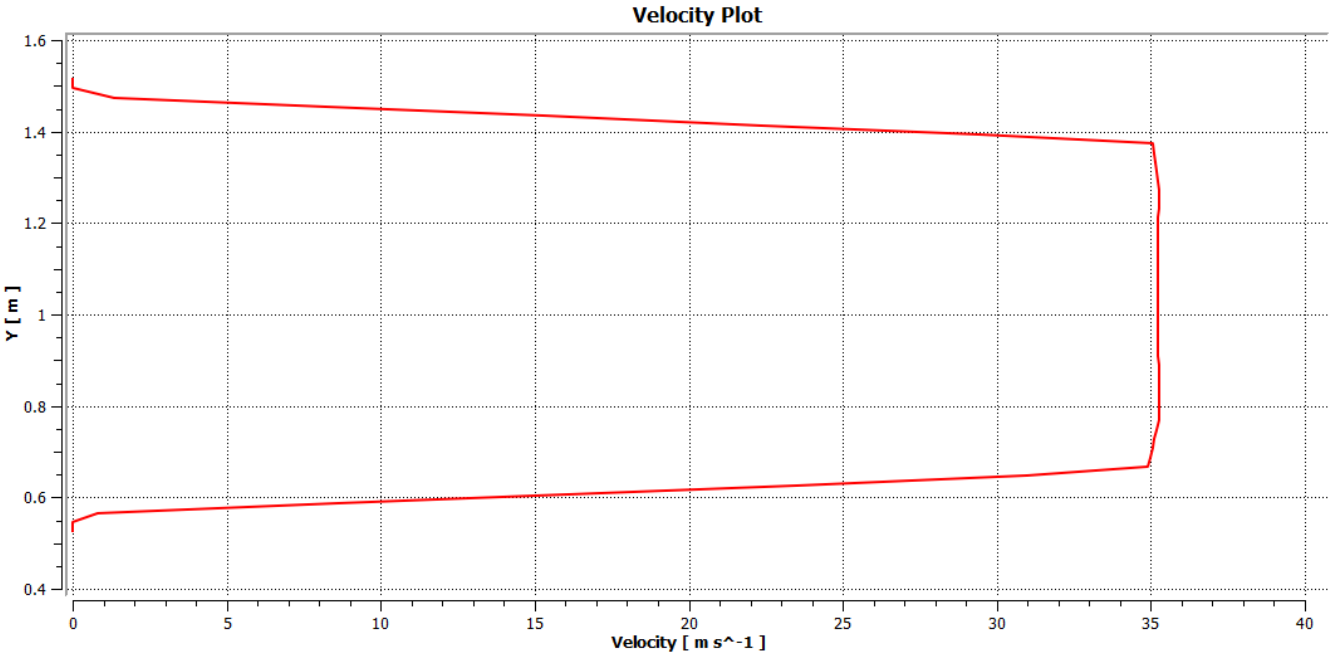

Chart 3.0 Velocity Distribution in Test Section for Closed Loop Wind Tunnel with C Vanes

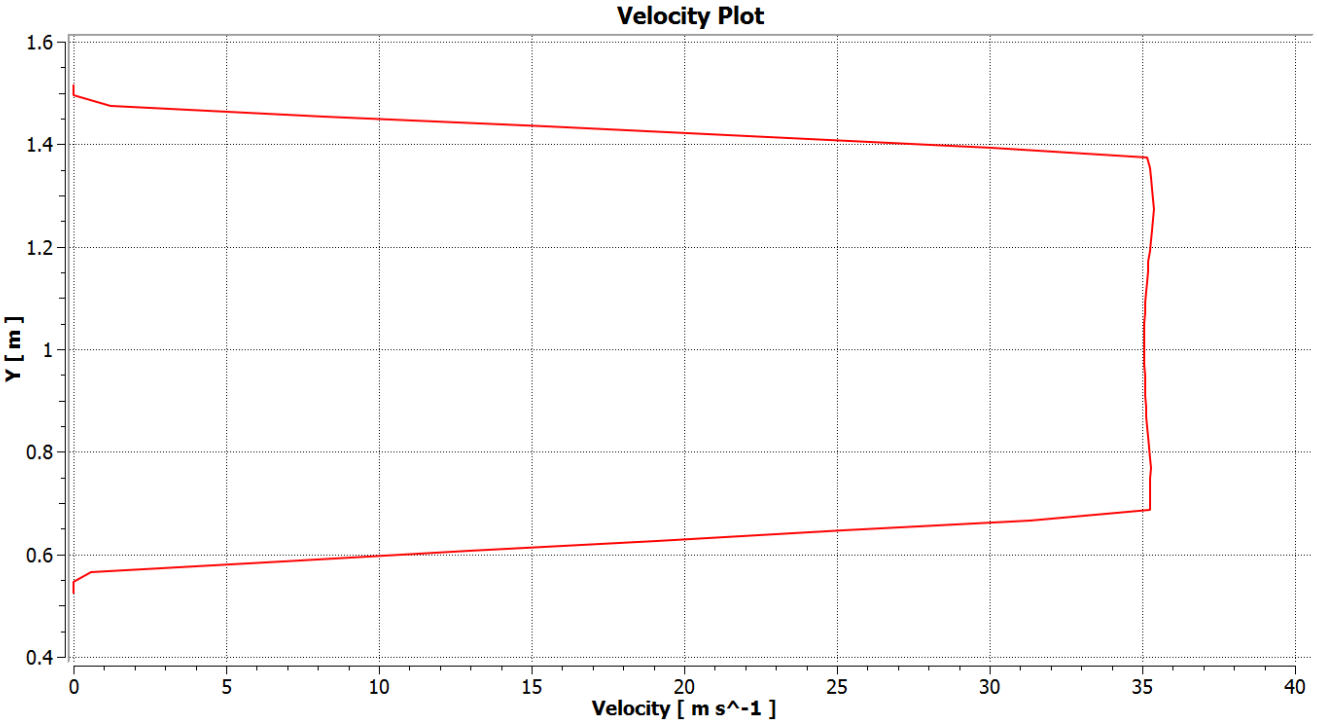

Chart 4.0 Velocity Distribution in Test Section for Closed Loop Wind Tunnel with NACA 6215 Airfoil Vanes

All the velocity chart plots show uniform velocity distribution with maximum value of 35m/s at the middle of test section and 0 m/s at the wall. This is consistence with the no slip boundary condition at the wall.

8 Discussion

8.1 Velocity

The velocity contours across the front plane of the wind tunnel is displayed in Figure# 18, 19, 20 and 21. The velocity distribution profile at the middle of test section is shown in chart# 1, 2, 3 and 4. The velocity profile chart plot show a valid solution alike that of the flow between two parallel plate, this is a strong proof to validate our computational model. It was observed that the velocity subsequently smoothed out as it passed through the guide vanes installed in the 90° turning vanes located at all four corners aided in reducing the re-circulation of the flow at the bends. The velocity vector field across the front plane of the wind tunnel is displayed in Figure# 26, 27,28 and 29 enhance the understanding of re-circulation with vorticity and stagnation velocity. Vorticity in the direction of the flow is like an obstacle which flow need to overcome to preserve continuity and therefore required more fan more. Therefore, in duct flow or any turbomachinery flow separation and vorticity are desired to be avoided to enhance efficiency or reduce power loss. Adding turning vanes proved to be desirable tool in wind tool to achieve this.

8.2 Pressure

The pressure contours across the front plane of the wind tunnel is displayed in Figure# 22, 23, 24 and 25. A distinctive pressure drop of 80 Pa was observed on thin 90 deg. bent vanes, however on C vanes and airfoil vanes pressure drop was reduced by the factor of 2 and 4 respectively. It was very hard to evaluate effectively the pressure losses however using probing tools in CFD post processing it was approximated that the pressure losses in corner 1 for case 2, 3 and 4. As streamed line body such as C-vanes and airfoil which directly the flow which abrupt change in flow direction pressure losses are reduce without compromising flow uniformity.

8.3 Turbulent Kinetic Energy

The turbulence kinetic energy across the front plane of the wind tunnel is displayed in Figure# 30, 31,32 and 33. The highest region of turbulence in the tunnel without any vanes were at the corner 3 and in test section. As the turning vanes were added the turbulence was reduced significantly. It was observed that the thin bent vent with longer trailing length vanes reduce turbulence however the airfoil vanes produces least turbulence in test section and more uniform flow. The vanes helped to dissipate the turbulent kinetic energy creating a less turbulent flow.

For case 4, due to calculation time and computational memory power, reduced number of element or increase maximum size of element, resulting flow behaviors is less refined than as predicted.

9 Conclusion

This project studied the effect of guide vanes in reducing the turbulent intensity and enhancing flow uniformity without sacrificing power. A comparison was done with the wind tunnel corners with and without incorporate turning vanes. Their aim is to reduce pressure loss possibly improve flow quality in the test section.

A crucial characteristic of wind tunnels is the flow quality inside the test chamber and the overall performances. Three main criteria that are commonly used to define them are: maximum achievable speed, flow uniformity and turbulence level. Therefore, the design aims of a wind tunnel, in general, is to get a controlled flow in the test chamber, achieving the necessary flow performance and quality parameters. In case of the Low speed wind tunnel, the requirements of those parameters are extremely strict, often substantially increasing the cost of facilities. But low turbulence and high uniformity in the flow are only necessary when, for example, laminar boundary layers have to be investigated. Therefore, the CFD design tool are very effective tools when we have to design best solution with cost consideration.

K-epsilon (k-ε) turbulence model is the most common model used in Computational Fluid Dynamics (CFD) to simulate mean flow characteristics for turbulent flow conditions. It is a two equation model which gives a general description of turbulence by means of two transport equations (PDEs). Direct solving of such PDE's for complex geometry are very complicated process, therefore with enhanced and faster computational techniques such case can be studied with less effort and cost effective using CFD Software. ANSYS Fluent is one of the leading industrial standard CFD software which was used for this project.

All models were created in more user friendly CAD software such as Solidworks which were later exported into ANSYS workbench for further analysis. Geometry acquisition and model post preparation was performed in Design modeler within workbench and CFD grade mesh were generated using with a minimum of time and effort. The Model was further analysis in Fluent to generated CFD data for post processing quantity such as velocity, pressure, turbulent kinetic energy and vorticity to study flow behaviors and optimize the model to design an effective model. The data collected from the simulation results indicate that a uniform laminar flow is maintained in the test section as desired by the streamlined body such as airfoil NACA 6215 with least corner pressure loss and provide least overall turbulence intensity. The project study successfully highlighted the capacity of using CFD techniques for characterizing the flow, turbulence and flow uniformity optimization within the entire physical domain of a closed-loop wind tunnel.

10 Reference

1. Mehta, R.D.; Bradshaw, P. Design rules for small low speed wind tunnels. *Aeronaut. J.* **1979**, *83*, 443–449.

2. Eckert W., Mort K. W. - Pope J. - Aerodynamic Design Guidelines and Computer Program for Estimation of Subsonic Wind Tunnel Performance National Aeronautics and Space Administration NASA TN D-8243, Washington, D.C., October, 1976.

3. Ahmed, N. A. Wind Tunnel - Designs and Their Diverse Engineering Applications. Rijeka, Croatia: INTECH, 2014. Print.

4. Pereira, Justin D. Wind Tunnels: Aerodynamics, Models, and Experiments. New York: Nova Science's, 2011. Print.

11 Appendix

1. Airfoil Matlab Code.

```
clear all
close all
clc


m=input('Enter the first of 4 digits of NACA airfoil: ');
p=input('Enter the second of 4 digits of NACA airfoil: ');
t=input('Enter the last two digits of 4 digits of NACA airfoil: ');
c=input('Enter the chord length: ');
n=input('Enter the number the iteration: ');

m=m/100;
p=p/10;
t=t/100;
i=1;
y_c(1,i)=0;


for x=0:c/n:c
    y_t(1,i)=t*c/0.2*(0.2969*sqrt(x/c)-0.1260*(x/c)-0.3516*(x/c)^2+0.2843*(x/c)^3-
0.1015*(x/c)^4);

    if (x>0 || x<=p*c)
        y_c(1,i+1)=(m*x/p^2)*(2*p-x./c);
    elseif (x>pc || x<=c)
        y_c(1,i)=((m*(c-x))/(1-p)^2)*(1+x/c-2*p);
    end
    dyc=(y_c(1,i+1)-y_c(1,i));
    dx=(c/n);
    theta(1,i)=atan(dyc/dx);
    x_u(1,i)=x-y_t(1,i)*sin(theta(1,i));
    x_l_c(1,i)=x+y_t(1,i)*sin(theta(1,i));
    y_u(1,i)=y_c(1,i)+y_t(1,i)*cos(theta(1,i));
    y_l_c(1,i)=y_c(1,i)-y_t(1,i)*cos(theta(1,i));
    z(1,i)=0;
    i=i+1;
  end

plot(x_u,y_u)
hold on
plot(x_l_c,y_l_c)
hold off
axis equal

for a=1:1:n+1
    x_l(1,a)= x_l_c(1,n+2-a);
    y_l(1,a)= y_l_c(1,n+2-a);
end
A = [x_u ;y_u; z];
B = [x_l; y_l ;z];
C=[A B];
C=C';
save airfoil.txt C -ASCII -tabs
```